May 2017

Evaluation of Durability of Existing Base Aggregates in Wisconsin Pavements

Mahmoud Akram Dakwar
University of Wisconsin-Milwaukee

EVALUATION OF DURABILITY OF EXISTING BASE AGGREGATES IN WISCONSIN PAVEMENTS

by

Mahmoud Dakwar

A Thesis Submitted in
Partial Fulfillment of the
Requirements for the Degree of

Master of Science
in Engineering

at
The University of Wisconsin-Milwaukee
May 2017

ABSTRACT

EVALUATION OF DURABILITY OF EXISTING BASE AGGREGATES IN WISCONSIN PAVEMENTS

by

Mahmoud Dakwar

The University of Wisconsin-Milwaukee, 2017
Under the Supervision of Professor Hani Titi

Highways are an integral part of modern societies, and high volumes of traffic are serviced by highways every hour of the day year-round. It is essential that transportation systems are strong, durable, and sustainable so that pavement damages and the loss of ride quality are minimized. The base-course aggregate layer acts as the foundation of the pavement system, and it supports the overlaying layers in the pavement structure. The objective of this research study was to evaluate the durability of existing base-course aggregates as they are impacted by external factors. Samples from fourteen sites were collected and additional data were obtained from other relevant studies. Aggregates from eleven sites out of the fourteen served in existing base layers. Durability and strength-related lab tests were performed on the collected samples, and the test results along with the data from other studies were analyzed by utilizing visual comparison statistical procedures and regression statistical methods.

For the eleven samples of aggregates that served in existing base-course layers, the results of the Micro-Deval abrasion test showed that two samples exceeded a recommended threshold limit of 18%, the results of the sodium sulfate soundness test showed that none of the samples exceeded the WisDOT threshold limit of 18%, and the

results of the aggregate absorption test showed that six of the samples exceeded a recommended threshold limit of 2%.

For the entire data used in the study, the results of regression analyses showed that the regression model MD% Loss = 5.62 × Absorption + 2.09 (with R^2 value of 0.86) can be used to make predictions and assess the performance quality of base-course aggregates accurately. The regression analyses results also demonstrated that the mass loss by sodium sulfate soundness test did not have strong correlations with either absorption or the mass loss by Micro-Deval abrasion.

TABLE OF CONTENTS

LIST OF FIGURES

LIST OF TABLES

ACKNOWLEDGEMENTS

I would like to give my deepest gratitude to Dr. Hani Titi for all your support, guidance, and help throughout my graduate work. Also, many thanks to Dr. Tabatabai and Dr. El Hajjar for your insight.

I would also like to extend special thanks to everyone who helped and supported me:

- Ahmed Shatnawi, Roonak Ghaderi, and Nicholas Coley for your companionship and help in the lab.
- John Condon, Michael Brown, and Robert Breske for all your help in the machine shop with fixing, fabricating, and lending equipment.
- Rahim Reshadi for all your help in the structures lab.

I would also like to thank Jiayan Nie, Majd Naji, Dan Van Gorden, Mike Kriefall, Lorne Forsyth, Azam Elyasigorji, Brian Mitchell, Te-An Wang, Saeed Yazdani, and Hua Liu for their friendship and support throughout the way.

Also, thank you so much to my parents Akram Dakwar and Siham Dakwar for all your love and support. Also, many thanks to my siblings Sarah Dakwar, Mohammed Dakwar, and Ahmed Dakwar for their patience and support.

CHAPTER 1

INTRODUCTION

Highways are an integral part of modern societies and high volumes of traffic are serviced by highways every hour of the day year-round. It is essential that transportation systems are strong, durable, and sustainable so that pavement damages and the loss of ride quality are minimized. The base-course layer is the foundation of the pavement surface, and it is important that the base-course layer is strong enough to support the upper layers of the pavement structure. The base-course aggregate layer supports the overlaying layers in the pavement structure, and traffic loads induced from bypassing traffic are transferred from the pavement surface down to the base layer. Having a quality base assists in reducing deformation and distresses in the pavement structure, thus keeping the road sustainable. To help maintain a quality roadway surface for a smooth drive as intended by design, the aggregates used in the construction of roadways should be durable and should also exhibit stable performance. It is a necessity that the base layer can adequately support the pavement system so that damages are minimized and so that the pavement system remains in good condition during its service life. Base-course aggregates may lose their durability over time due to external factors such as traffic loading and freeze-thaw action.

This research intends to evaluate the durability of existing base-course aggregates as they are impacted by external factors. The performance quality of aggregates is an indicator of their durability.

1.1 Background

The Wisconsin Department of Transportation (WisDOT) inspects and reviews its pavement design process annually to control the damages to roadways. Every year, WisDOT assesses the soil and pavement materials currently in place to integrate them within the pavement design process. Borings are performed in order to acquire samples of soil and pavement materials because they are the core of the pavement evaluation process. A closer look at the samples obtained from the borings has revealed the occurrence of degradation of base-course aggregates over time. To address this issue, the DOT identified the physical and chemical breakdown of individual aggregates, freeze-thaw action, and the infiltration of subgrade materials as the three main contributing factors to base-course aggregate deterioration.

Within the context of the research conducted for this thesis, samples of base-course aggregate were collected from multiple project sites in Wisconsin and tested by performing a series of various experiments for the purpose of assessing base aggregate durability and the ability to perform under existing pavements.

1.2 Problem Statement and Objective

Durability is an important characteristic of aggregates serving in base layers under existing pavements. The objective of the research was to assess the durability of aggregates that have been in use in existing roadways in Wisconsin. Samples were collected from fourteen sites in Wisconsin for this study and the data analysis accounted for data obtained from the collected samples along with data obtained from relevant

studies. Field and lab testing employed for this study included a selected number of commonly used durability and strength tests.

1.3 Overview of Methodology

In order to explore the performance quality of base-course aggregates, samples of base-course aggregate were collected from various project sites in Wisconsin, field and lab testing were conducted on specimens, data were collected from the tests performed, additional data sets were obtained from relevant studies, and statistical analyses were employed for data analysis.

Field testing consisted of the Dynamic Cone Penetration (DCP) test, and lab testing included sieve analysis, specific gravity and absorption of aggregates, the Micro-Deval abrasion test, the sodium sulfate soundness test, standard laboratory compaction, and the California Bearing Ratio (CBR) test. The DCP test is used to determine the penetration per blow through the layers in the pavement system that were involved in the test. The purpose of sieve analysis is to determine the grain-size distribution of the sample. Standard laboratory compaction is used to determine a relationship between moisture content and unit weight in order to determine the optimum moisture content which corresponds to the maximum dry unit weight. The specific gravity and absorption test is used to determine the oven-dry specific gravity, saturated-surface-dry specific gravity, apparent specific gravity, and water absorption of aggregates. The Micro-Deval abrasion test measures the percentage of mass lost after introducing an abrasive charge while in the presence of water. The sodium sulfate soundness test measures the

percentage of mass lost after subjecting the samples to multiple two-stage cycles where the first stage involves immersing specimens in sodium sulfate solution for a period of time and the second stage involves drying them in the oven. The CBR test was used as a measure of strength. The test methods used along with their corresponding ASTM designations are displayed in Table 1.1.

Table 1.1: Table displaying the test methods that were employed and their corresponding ASTM Designations.

ASTM Designation	AASHTO Designation	Test Method
D6951	N/A	Standard Test Method for Use of the Dynamic Cone Penetrometer in Shallow Pavement Applications
C136	T27	Sieve Analysis of Fine and Coarse Aggregates
C117	T11	Materials Finer than 75-mm (No. 200) Sieve in Mineral Aggregates by Washing
D698	T99	Laboratory Compaction of Soil Using Standard Effort
C127	T85	Relative Density (Specific Gravity) and Absorption of Coarse Aggregate
D6928	N/A	Resistance of Coarse Aggregate to Degradation by Abrasion in the Micro-Deval Apparatus
D7428	N/A	Resistance of Fine Aggregate to Degradation by Abrasion in the Micro-Deval Apparatus
C88	T104	Soundness of Aggregates by Use of Sodium Sulfate or Magnesium Sulfate
D1883	T93	Test Method for California Bearing Ratio (CBR) of Laboratory-Compacted Soils Standard

Statistical analyses included creating bar graphs to compare the results to specific threshold limits depending on the test and developing regression models. The bar graphs were utilized by making a comparison of the data obtained from the Micro-Deval abrasion, sodium sulfate soundness, and aggregate absorption test for the collected samples with specific threshold limits. The outcomes were used to draw conclusions

about the durability of the aggregates in terms of their performance quality. The strategy in addressing the research investigation by using regression analysis was to compare various regression models to select a model that could accurately predict the performance quality of aggregates and make inferences about the performance quality of Wisconsin aggregates.

1.4 Outline of Thesis

The structure of this thesis organizes the content into six chapters. Chapter One introduces the background, problem statement, and the objective of the research. Chapter Two includes reviews of relevant literature pertaining to the various tests performed for the thesis in addition to related studies. Chapter Three discusses the methodology used to approach the research question. Chapter Four presents the results obtained from the samples collected for this study and Chapter Five provides the interpretation and analysis of the results obtained from the samples collect for this study and data obtained from related studies. Chapter Six summarizes the conclusions and findings of the research.

CHAPTER 2

LITERATURE REVIEW

This chapter presents relevant literature about durability and strength-related lab tests that were performed for the study in addition to studies pertaining to this research. Lab testing includes brief explanations and the significance of each test used. Related studies include findings of studies involving the investigation base-course aggregate durability.

2.1 Resistance to Abrasion by Micro-Deval

The Micro-Deval abrasion test is used to estimate the abrasion-resistance and durability of aggregates. The aggregate specimen is placed into a container along with a combination of steel balls and water. The sample is then subjected to grinding and abrasion by the steel balls and water while the container is revolved in the Micro-Deval apparatus. The specimen is dried to constant mass in an oven and the percentage of mass lost due to the test is determined (ASTM, 2016).

The inclusion of water in this test makes it so that it reflects field performance more accurately than the Los Angeles abrasion (L.A. abrasion) test does, which is a commonly used test for estimating aggregate durability. The results from the Micro-Deval test also serve as a good indicator of the durability of aggregates. While the Micro-Deval test is a good quality-control measure, it is worthwhile to note that it has not been incorporated by WisDOT (Weyers et al., 2005).

Different sources have proposed and implemented different Micro-Deval abrasion acceptance limits for coarse aggregates. Kandhal and Parker suggested a limit of 18% for coarse aggregates (Kandhal and Parker, 1998). The Canadian Standards Association set a Micro-Deval abrasion limit of 20% for coarse aggregates (Weyers et al., 2005). A recommendation made by Woodward was to use different Micro-Deval abrasion limits depending on the minerology of the aggregates (1995).

2.2 Soundness by Sodium Sulfate

The sodium sulfate soundness test is used to simulate freeze-thaw conditions. The test is composed of five cycles, each cycle consisting of a freezing stage and thawing stage. Each cycle is composed of two stages: 1) Placing the specimen in sodium sulfate solution; and then 2) Oven-drying the specimen to constant mass. The formation of crystals within the solution is intended to simulate freezing, and the heat from the oven is intended to simulate thawing. After the five cycles are completed, the mass loss of aggregate is determined as a percentage (ASTM, 2016).

It is also noteworthy to mention that this test is used by WisDOT to help assess the durability of aggregates. A typical threshold values for sodium sulfate soundness is 12%. One of the issues with the sodium sulfate soundness test is that it lacks precision because there may be inconsistencies between results. Because of this, aggregates should not be outright rejected based solely from the results of this test (Weyers et al., 2005).

2.3 Specific Gravity and Absorption

Specific gravity and absorption are typical properties used to assess aggregates. Specific gravity is the ratio of mass of an aggregate to the mass of a volume of water equal to the volume of the aggregate particles. Absorption is an increase in mass due to the water absorbed in the pores of a material. A high absorption value may indicate that an aggregate is not durable. (ASTM, 2016). While specific gravity and absorption are typically used as general characteristics of aggregates, absorption can also be used to indirectly predict the freeze-thaw durability of aggregates. An acceptance limit of 2% was recommended by Pigeon and Pleau (1995).

2.4 California Bearing Ratio

The California Bearing Ratio test is a load-deformation test that is sometimes used to assess the strength of soil and aggregates for pavement design. The CBR is defined as the ratio of the test load to the standard load for a specified penetration depth. For a given penetration depth, the penetration resistance of the piston into a standard sample of crushed stone for a given penetration depth is defined as the standard load (Jigar & Patel, 2013).

2.5 Correlation between DCP and CBR

The soaked CBR test requires the specimen to be soaked for a period of four days. The soaked CBR test compromises the location of the actual site since lab conditions do not necessarily reflect field conditions. However, the DCP test is a field test that can be used to predict the CBR. Attempts have been made to correlate the penetration rate

obtained from the DCP test to the CBR. The DCP is a field test rather than a lab test, is much less time consuming than the CBR test, and can easily be repeated more frequently in order to get multiple sets of results for consistency purposes. Despite the simplicity of using the DCP test to assess the strength of aggregates, it should not be used as a replacement for the CBR test because the correlation between DCP and CRB do not necessarily indicate the actual CBR value of the material tested (Wijekoon, 2014).

One of the correlations between the DCP test results and CBR was developed by Kleyn (1975). From the results obtained in his study, the following correlation between the penetration rate and CBR was established: $\log(CBR) = 2.62 - 1.27\log(PR)$. This can be rearranged as $CBR = \frac{10^{2.62}}{(PR)^{1.27}}$, and then ultimately as $CBR = \frac{417}{(PR)^{1.27}}$. In this equation, CBR represents the California Bearing Ratio and PR represents the penetration rate (Titi et al., 2012).

2.6 Testing Methods to Determine Durability of Wisconsin Aggregate Resources

Weyers et al. (2005) investigated testing methods that have been used to estimate aggregate durability were investigated. The intention was to include testing methods that can more accurately estimate durability and get rid of inefficient testing methods. The testing methods that were investigated include vacuum absorption, Micro-Deval abrasion, L.A. abrasion, sodium sulfate soundness, freeze-thaw soundness, unconfined freeze-thaw, etc. Based on the study, one of the recommendations was to incorporate the Micro-Deval abrasion test into any aggregate durability testing protocol. An important finding of the study was that the Micro-Deval abrasion test is a better indicator of durability than the

L.A. abrasion test, while the L.A. abrasion test is a better indicator of strength (Weyers et al, 2005).

Although aggregate absorption does not have a direct relation with aggregate quality, it can serve as an indirect indicator of aggregate durability. It was found that almost half of aggregates that were tested by Micro-Deval abrasion would be rejected when using the recommended threshold limit of 18%. However, a mass loss limit ranging from 25% to 30% was considered as a reasonable recommendation as a threshold limit for Wisconsin aggregates. It was stated that a commonly accepted threshold limit for sodium sulfate soundness is 12%. While an advantage of the sodium sulfate soundness test lies in its capability to identify poor performing aggregates, a disadvantage is that it does not have the ability to detect certain types of aggregates with poor performance. Another disadvantage of the sodium sulfate soundness test is that it does not produce consistent results (Weyers et al., 2005).

The testing methods discussed in “Testing Methods to Determine Durability of Wisconsin Aggregate Resources" (Weyers et al., 2005) that were relevant to this thesis were the absorption test, Micro-Deval abrasion test, and sodium sulfate soundness test. Additionally, the data from the study by Weyers et al. (2005) related to absorption, Micro-Deval, and sodium sulfate soundness were obtained and implemented for regression analysis in this study.

2.7 Investigation of Testing Methods to Determine Long-Term Durability of Wisconsin Aggregates

Tabatabai et al. (2013) investigated 12 aggregates that were identified as having marginal or poor performance were investigated for their durability characteristics. Micro-Deval abrasion, L.A. abrasion, sodium sulfate soundness, unconfined freeze-thaw, and absorption were performed on those aggregates. Additionally, the Wisconsin historical database was examined to recommend more reasonable threshold limits. The value ranking at the 75th percentile was selected as an acceptable limit for each test. The recommended threshold limits were 2.3% for absorption of coarse aggregates and 6% for sodium sulfate soundness. For Micro-Deval, 16% and 18% were mentioned, but neither was ranked at the 75th percentile. Multi-variable regression models were developed for determining the output of the Micro-Deval test. Additionally, the unconfined freeze-thaw test was recommended as a required test for aggregate durability testing protocol because it does not correlate with the other parameters of the multi-regression models (Tabatabai et al, 2013).

The data from the Micro-Deval abrasion, sodium sulfate soundness, and absorption tests of the twelve investigated poor aggregates from the study by Tabatabai et al. (2013) were obtained and incorporated into the regression analyses that were conducted for this thesis. The addition of these aggregates helped in obtaining more data for more reliable results.

CHAPTER 3

METHODOLOGY

This chapter explains the methods and procedures used to carry out the study, including the selection of project sites, sample collection, field testing, lab testing, and the statistical analysis of results. The tests employed for this study are summarized in Table 3.1

Table 3.1: Tests conducted on samples.

Project Site	DCP	Grain-Size Distribution	Laboratory Compaction	Specific Gravity & Absorption	Micro-Deval	Sodium Sulfate Soundness	CBR
STH 33	✓	✓	✓	✓	✓	✓	✓
STH 162	✓	✓	✓	✓	✓	✓	✓
STH 36-S1-B	✓	✓	✓	✓	✓	✓	✓
STH 36-S2-B		✓	✓	✓	✓	✓	✓
STH 36-S1-G	✓	✓		✓	✓	✓	✓
STH 36-S2-G	✓	✓	✓	✓	✓	✓	✓
STH 36-S3-G	✓	✓		✓	✓	✓	✓
STH 180	✓	✓	✓	✓	✓	✓	✓
USH 53	✓	✓	✓	✓	✓	✓	✓
I 94-S1		✓	✓	✓	✓	✓	✓
I 94-S2	✓	✓		✓	✓	✓	✓
Jefferson SH-18			✓	✓	✓	✓	
STH 33 Saukville		✓	✓	✓	✓	✓	
USH 45		✓	✓	✓	✓	✓	✓

3.1 Site Selection

The criteria used for the selection of sites considered three aspects: 1) Different geographical locations in Wisconsin; 2) Aggregates having served in base-course layers as virgin aggregates; and 3) Pavement type. The project sites selected were located in various geographic regions scattered throughout Wisconsin. An emphasis was placed on aggregates that served in existing base-course layers as virgin aggregates. Also, an emphasis was placed on sites with asphalt pavement. Twelve sites were selected for this study in such a way that nine of them contained aggregates from existing base-course layers and the other three contained newly placed virgin aggregates. The nine site that consisted of existing base-course layers were STH 33, STH 162, STH 36 (Site #1, Site #2, and Site #3), STH 180, USH 53, and I 94 (Site #1 and Site #2). The three sites that consisted of newly placed virgin aggregates were Jefferson SH-18, STH 33-Saukville, and USH 45.

It is worth noting that all of the sites selected consisted of asphalt pavement except for USH 53, which consisted of concrete pavement. Twelve different sites were selected, and they are presented on the map in Figures 3.1 (a) and 3.1 (b). Additionally, the GPS coordinates of the sites containing aggregates from existing base-course layers are displayed in Table 3.2. Aerial views of the project sites containing aggregates from existing base-course layers are shown in Figure 3.2 (a) through Figure 3.2 (h). The aggregate type of each sample collected is shown in Table 3.3. The thicknesses and ages of the pavement and base-course aggregate layers are shown in Table 3.4.

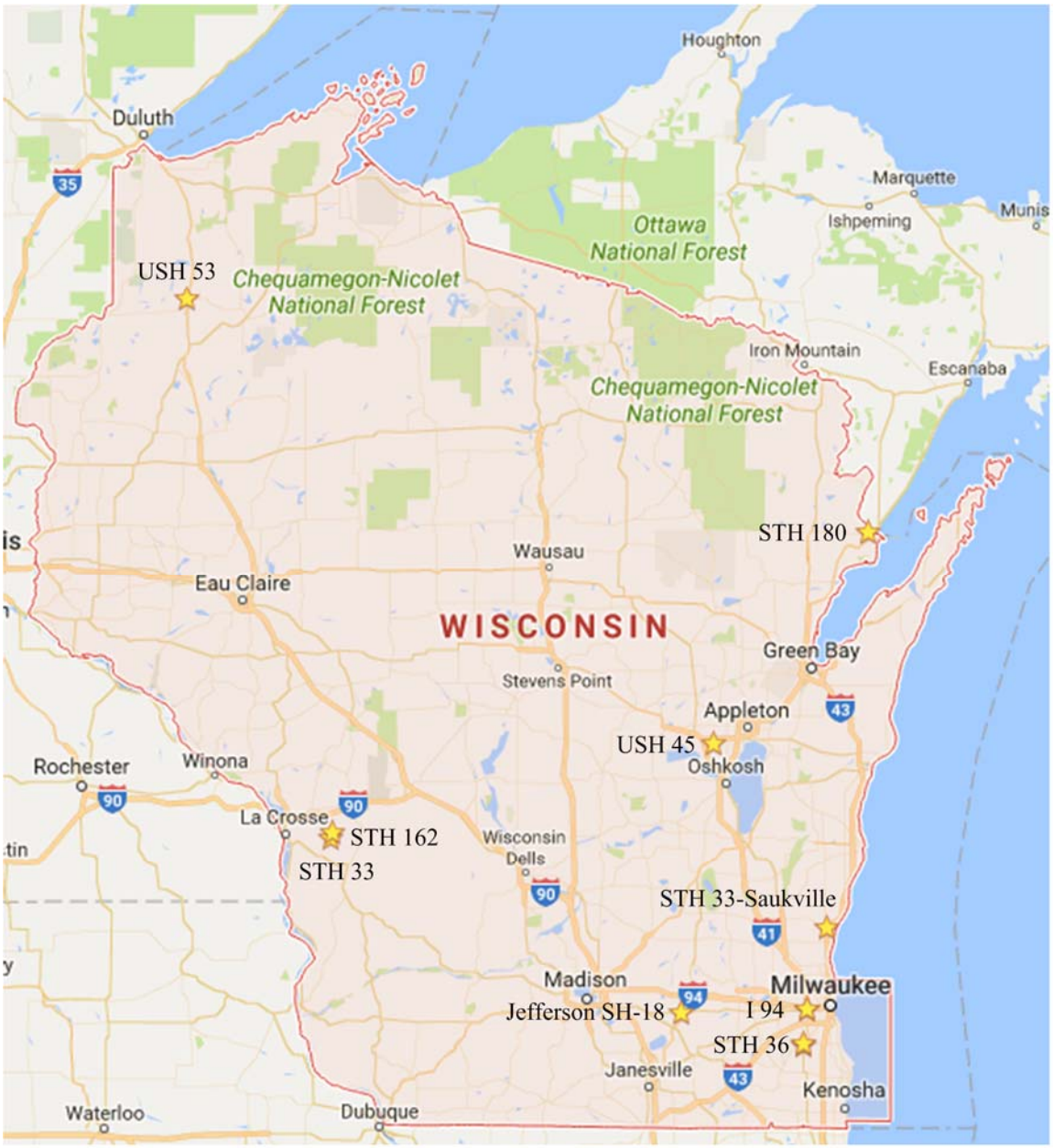

Figure 3.1 (a): Map showing the locations of the project sites that were investigated for this study (Google Maps, 2017).

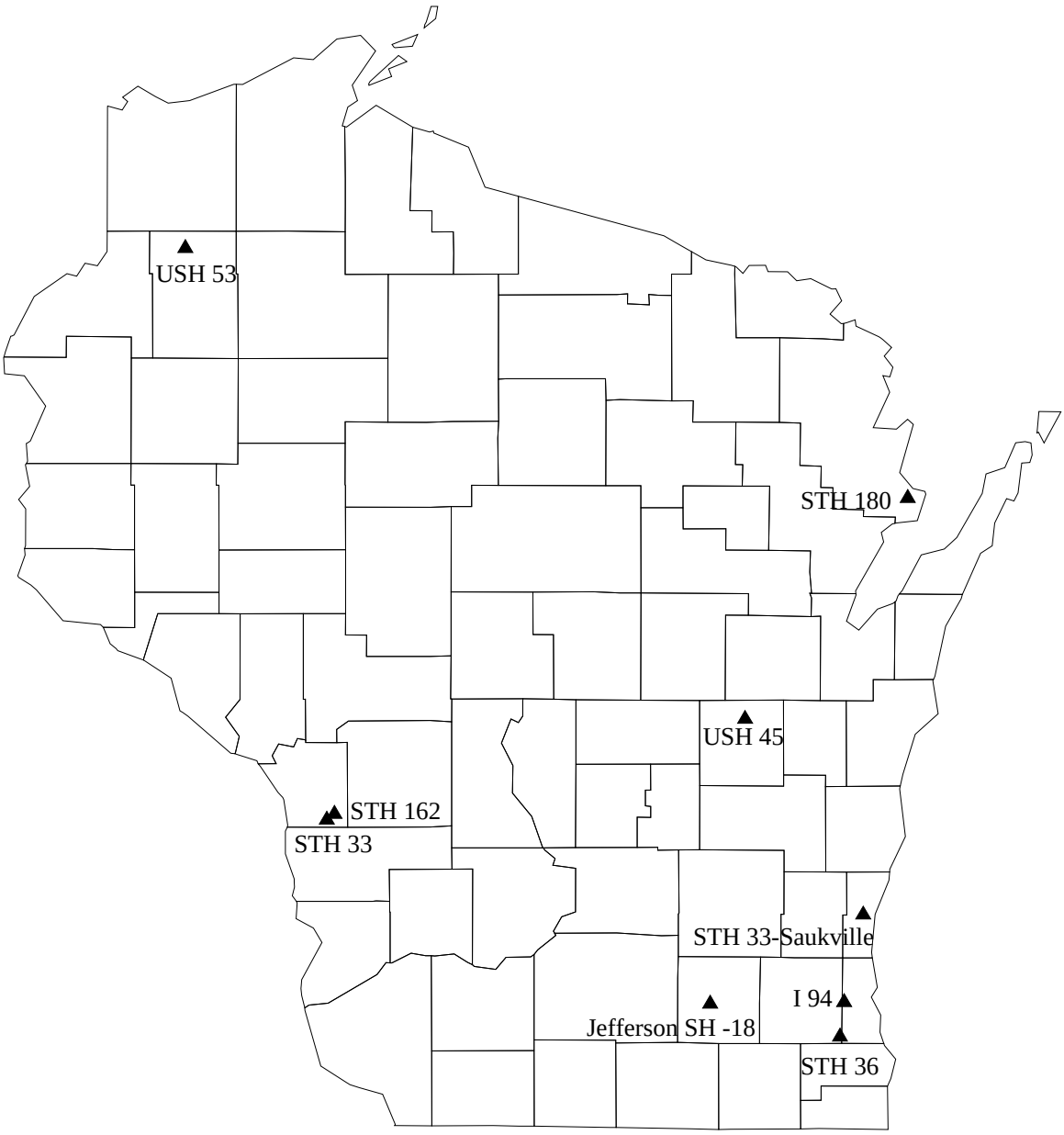

Figure 3.1 (b): Map showing the locations of the project sites that were investigated for this study.

Table 3.2: GPS Coordinates of project sites.

Project Site	GPS Coordinates
STH 33	43.786923, -90.957798
STH 162	43.808499, -90.948446
STH 36-S1	42.866682, -88.076050
STH 36-S2	42.869295, -88.071979
STH 36-S3	42.869295, -88.071979
STH 180	45.111916, -87.671783
USH 53	46.102265, -91.836875
I 94-S1	43.028210, -88.044826
I 94-S2	43.028210, -88.044826

Figure 3.2 (a): Map displaying the site location on STH 33 (Google Maps, 2017).

Figure 3.2 (b): Map displaying the site location on STH 162 (Google Maps, 2017).

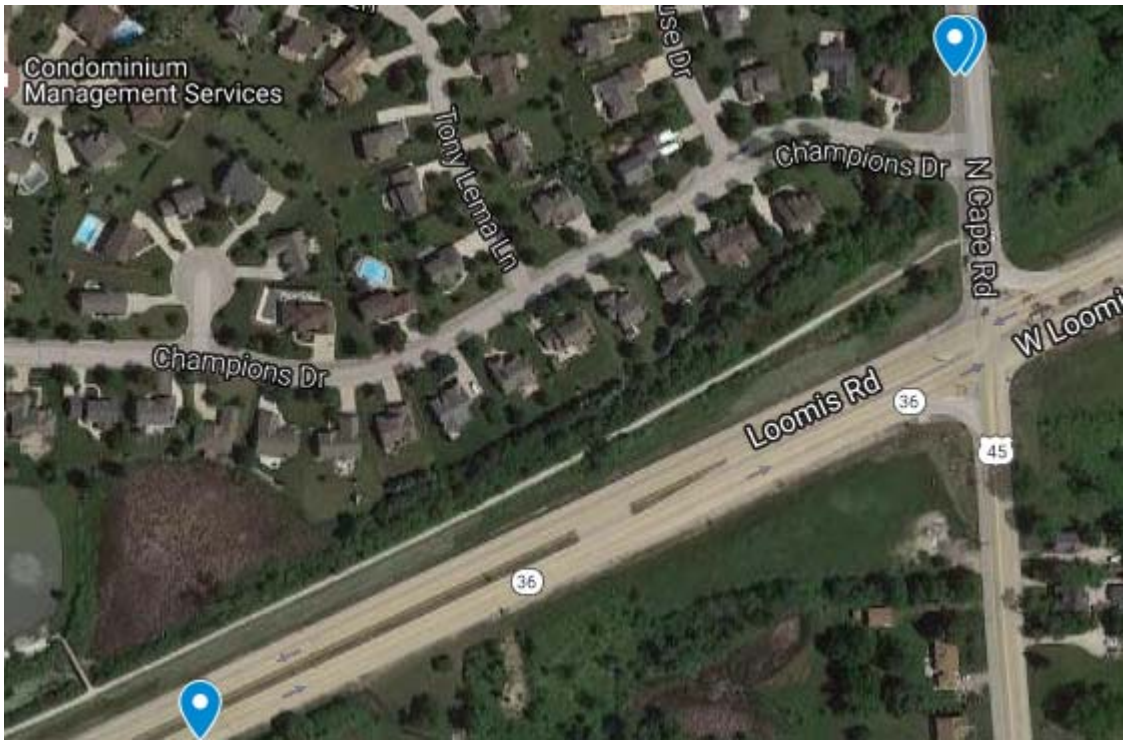

Figure 3.2 (c): Map displaying the site locations of STH 36 (Google Maps, 2017).

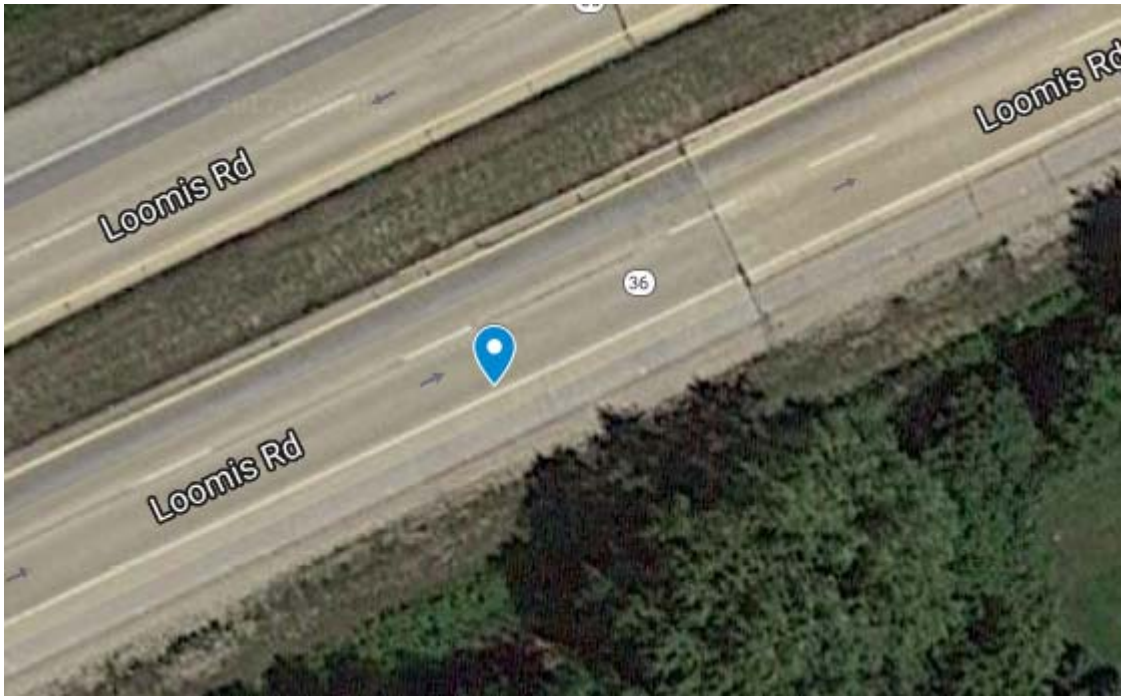

Figure 3.2 (d): Map displaying the site location on STH 36-S1 (Google Maps, 2017).

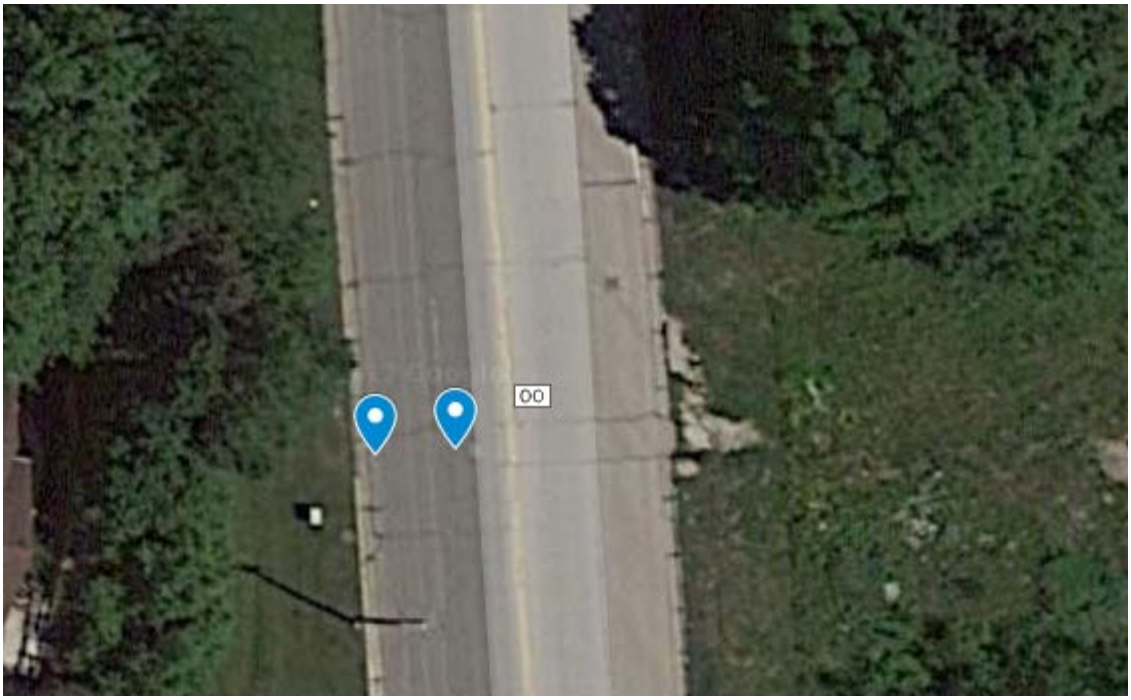

Figure 3.2 (e): Map displaying the site locations on STH 36-S2 and STH-S3 (Google Maps, 2017).

Figure 3.2 (f): Map displaying the site location on STH 180 (Google Maps, 2017).

Figure 3.2 (g): Map displaying the site location of USH 53 (Google Maps, 2017).

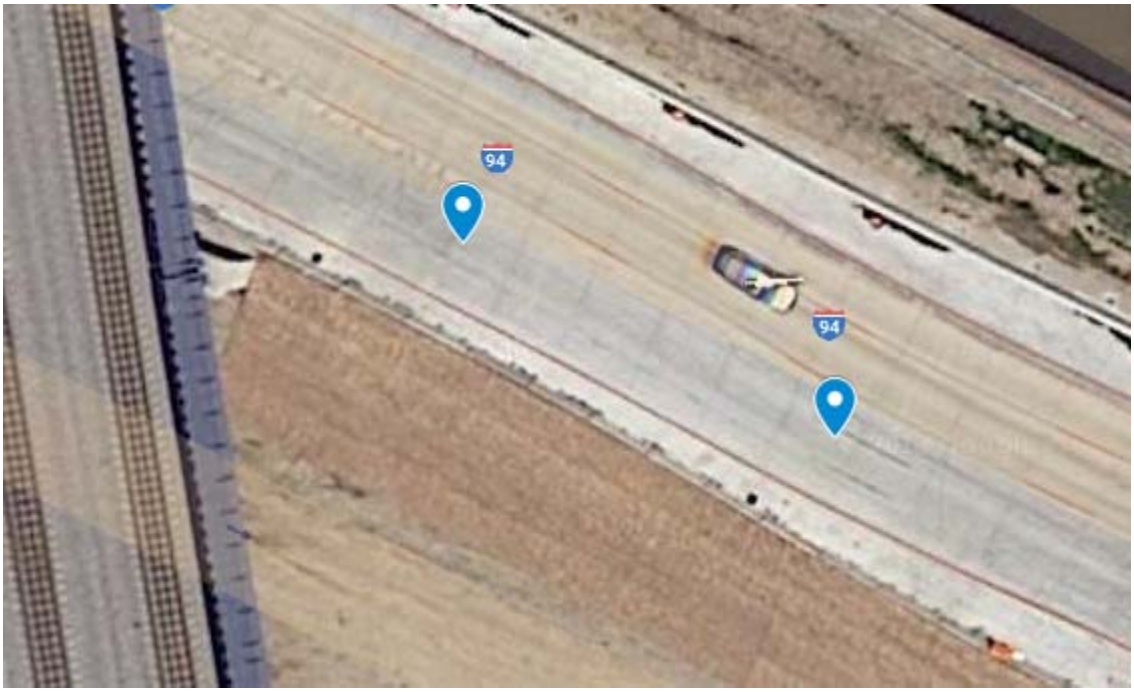

Figure 3.2 (h): Map displaying the site locations of I 94-S1 and I 94-S2 (Google Maps, 2017).

Table 3.3: Type of aggregate collected from each site.

Project Site	Aggregate Type
STH 33	Virgin/Existing
STH 162	Virgin/Existing
STH 36-S1-B	Virgin/Existing
STH 36-S2-B	Virgin/Existing
STH 36-S1-G	Virgin/Existing
STH 36-S2-G	Virgin/Existing
STH 36-S3-G	Virgin/Existing
STH 180	Virgin/Existing
USH 53	Virgin/Existing
I 94-S1	Recycled/Existing
I 94-S2	Recycled/Existing
Jefferson SH-18	Virgin/Newly placed
STH 33-Saukville	Virgin/Newly placed
USH 45	Virgin/Newly placed

Table 3.4: Thickness and age of the samples collected from each project site from WisDOT plans, field measurements, and as predicted from the DCP test.

Project Site	Surface			Base-Course			
	Age (yrs)	Thickness (in)		Age (yrs)	Thickness (in)		
		WisDOT	Field		WisDOT	Field	DCP
STH 33	20	2	N/A	86	10	N/A	10
	85	4	N/A	N/A	N/A	N/A	N/A
STH 162	N/A	12	N/A	86	10	N/A	10
STH 36-S1	N/A	4-11	N/A	18	6	N/A	N/A
	N/A	0-11	N/A	18	4	11	11
	N/A	N/A	N/A	18	12	15.5	15
STH 36-S2	N/A	4-11	4	18	6	8	N/A
	N/A	0-11	9	18	4	6	6
STH 36-S3	N/A	4-11	4	18	6	8	N/A
	N/A	0-11	9	18	4	6	6
STH 180	19	1.75	N/A	79	3	N/A	4
	79	4	N/A	N/A	N/A	N/A	N/A
USH 53	18	9	N/A	18	6	N/A	6
I 94-S1	N/A	7.5	8	56	13	11	N/A
I 94-S2	N/A	7.5	8	56	13	11	11
Jefferson SH-18	N/A	N/A	N/A	0	N/A	N/A	N/A
STH 33-Saukville	N/A	N/A	N/A	0	16.5	N/A	N/A
USH 45	N/A	N/A	N/A	0	6	N/A	N/A

3.2 Sample Collection

The base-course aggregate layer was the point of interest of the project sites with relation to this research. From the nine selected sites with existing base-course layers, eleven samples of base-course aggregate were collected with the aid of basic tools such as shovels and pick-axes to dig down to the base-course aggregate layer. The material was then obtained from the base-course aggregate layer and placed into 5-gallon buckets. On average, three buckets of each sample were collected, and thirty-three samples were collected in total. The three virgin aggregate samples were obtained from a previous study, where one bucket of each sample was obtained. Ultimately, thirty-six buckets comprised the collected samples for this study.

3.3 Field and Lab Testing

A series of field and lab tests were carried out to obtain results where conclusions about the research question can be drawn. The Dynamic Cone Penetration test was the only test that was conducted in the field. The lab tests conducted were sieve analysis, standard laboratory compaction, specific gravity and absorption, Micro-Deval test, sodium sulfate soundness test, and the California Bearing Ratio test. All lab testing was performed in the Soil Mechanics Lab at the University of Wisconsin-Milwaukee (UWM) with the exception of the CBR test which was performed in the Structural Lab at UWM.

3.3.1 Dynamic Cone Penetration Test

The DCP test was used to determine the penetration per blow through the layers in the pavement system that were subjected under the test. The instrument used for this test was the Dynamic Cone Penetrometer which consists of a drive-rod, a hammer, an anvil, a cone-tip, and a vertical scale. The cone-tip was attached to the bottom of the drive rod and the Dynamic Cone Penetrometer was situated on top of the base-course aggregate layer. To run the test, the hammer was lifted to the top of the device and then allowed to freely fall until it hit the anvil. When the load was imparted to the anvil, the drive-rod was driven down into the aggregate layer. The vertical scale was used to measure the depth that the rod was driven down into the layer, which is referred to as penetration depth. The data obtained in the field was used to calculate the penetration rate. The penetration rate was calculated by subtracting successive depths (note that the penetration rate for the first blow is equal to the depth for the first blow). The penetration

depth (with respect to the initial position of the cone tip) was plotted against the penetration rate.

Additionally, the CBR values were predicted from the penetration rate at the corresponding depths by using a rearranged version of Kleyn's (1975) equation that amounts to:

$$CBR = \frac{417}{(PR)^{1.27}} \tag{3.1}$$

It is important to note that the penetration rate needs to be in units of mm/blow when using equation (3.1). After the CBR was calculated at each depth, a graph of the CBR versus the penetration depth was produced. The CBR versus penetration depth graph was divided up into layers based on the nature of the graph in terms of patterns and abrupt changes in those patterns. The thickness of the base-course layer was estimated from the graph. The average of the CBR values that were previously calculated for the assumed base-course layer was taken to estimate the CBR value of the entire base-course layer.

3.3.2 Sieve Analysis

Sieve analysis was used to determine the grain-size distribution of the base-course aggregate specimens. First, the sample was oven-dried to constant mass at 230 °F. Then quartering was used to reduce the sample into a test sample that was at least 15 kilograms. The purpose of this was to prepare a test sample that was representative of the sampled project site location.

Next, the sample was washed over a No. 200 sieve so that material finer than the No. 200 sieve would pass through the opening of the sieve. Then the sample was oven-dried to constant mass once again.

Afterwards, a set of sieves were stacked with the sieve that had the largest mesh opening size at the top. Sieves were stacked from top to bottom in descending order according to their mesh opening sizes, with a pan placed at the bottom. The sieve sizes used were in compliance with the WisDOT specifications for the grain-size distribution of base-course aggregate layers. The selected sieve sizes were as follows: 1.25”, 3/4 “, 3/8”, No. 4, No. 10, No. 40, and No 200.

The stacked sieves were then placed onto a sieve shaker and agitated to allow as many grains to pass through the sieve openings that they are smaller than. The mass retained on each sieve was measured on a weighing scale. The mass retained was used to calculate the percentage of particles passing through each sieve. The grain-size was plotted versus the percentage of material passing each sieve to obtain the graph of the grain-size distribution.

3.3.3 Micro-Deval Abrasion Test

The Micro-Deval abrasion test measures the resistance of aggregates to abrasion. As a brief overview of the test, a specimen is placed into a container in addition to stainless steel balls and water. The container is placed into the Micro-Deval apparatus and revolved to produce an abrasive charge. Because of the abrasive charge, the sample

degrades. Water is used in the test because aggregates are more susceptible to abrasion in the presence of water. The Micro-Deval abrasion test was run on both coarse aggregates and fine aggregates. The steps for the Micro-Deval abrasion test are explained for the coarse aggregate specimen. The steps for the fine aggregate specimen are the same except that the sieve sizes and masses retained, volume of water, mass of the steel balls, and number of revolutions were different from those used for coarse aggregates.

The coarse aggregate specimen consisted of the following fractions: 375 grams passing the 3/4" sieve and retained on the 5/8” sieve, 375 grams passing the 5/8” sieve and retained on the 1/2” sieve, and 750 grams passing the 1/2" sieve and retained on the 5/8” sieve. For a few of the coarse aggregate specimens, the following gradation was used: 750 grams passing the 1/2" sieve and retained on the 3/8" sieve, 375 grams passing the 3/8” sieve and retained on the 1/4" sieve, and 750 grams passing the 1/4" sieve and retained on the No. 4 sieve. The initial weight of the coarse specimen was 1500 grams. The specimen was placed into the Micro-Deval container and 2 liters of water were added to the container. The specimen was immersed in water for at least one hour. Then 5 kilograms of steel balls were added into the container. The container was then placed into the Micro-Deval apparatus. The apparatus had a revolution counter, so the number of revolutions was set to 12,000 revolutions (10,500 revolutions for the alternate gradation). The container revolved at a rate of 100 revolutions per minute. The revolving of the container lasted for approximately two hours, and the container was taken out of the apparatus once the revolutions were completed.

The coarse aggregate specimen was then poured out of the container over a No. 4 sieve super-imposed onto a No. 16 sieve, and the specimen was washed over the sieves. Then the steel balls were removed with a magnet. Next, the sample was oven dried at a temperature of 230 °F for 24 hours. The sample was weighed afterwards, and the final mass was recorded. The percent loss (% Loss) was then calculated using the equation $\%Loss = \frac{A-B}{A} \times 100\%$, where A is the initial mass of the specimen and B is the final mass.

For the fine aggregates, the specimen consisted of the following fractions: 50 grams passing the No.4 sieve and retained on the No. 8 sieve, 125 grams passing the No. 8 sieve and retained on the No. 16 sieve, 125 grams passing the No. 16 sieve and retained No. 30 sieve, 100 g passing the No. 30 sieve and retained on the No. 50 sieve, 75 grams passing the No. 50 sieve and retained on the 100 sieve, and 25 grams passing the No. 100 sieve and retained on the No. 200 sieve. The initial mass of the fine specimen was 500 grams. The specimen was placed into the Micro-Deval container and 0.75 liters of water were added to the container. The specimen was immersed in water for at least one hour. Then 1.2 kg of steel balls were added into the container. The container was then placed into the Micro-Deval apparatus. The number of revolutions was set to 1500. The container revolved at a rate of 100 revolutions per minute. The revolving of the container lasted for approximately 15 minutes, and the container was taken out of the apparatus once the revolutions were completed.

The fine aggregate specimen was then poured out of the container over a No. 4 sieve super-imposed onto a No. 200 sieve, and the specimen was washed over the sieves. Then the steel balls were removed with a magnet. Next, the sample was oven dried at a temperature of 230 °F for 24 hours. The sample was weighed afterwards, and the final mass was recorded. The percent loss was then calculated by using the same equation that was used to determine the percent loss of the coarse aggregate specimen.

3.3.4 Sodium Sulfate Soundness Test

The sodium sulfate soundness test was used to simulate freeze-thaw cycles. For this test, each sample was divided into seven specimens. The test consisted of five cycles and each cycle was performed in two stages 1) Placing the specimen in a container of sodium sulfate solution; and then 2) Oven-drying the specimen to constant mass.

The sodium sulfate solution was prepared by mixing anhydrous salt (sodium sulfate) with distilled water. 215 grams of anhydrous salt were added for every liter of distilled water. The solution was mixed by using a mixing attachment connected to a power drill. The solution was left to settle for a minimum of 48 hours, and then the specific gravity was measured to ensure that it fell between the range of 1.151 and 1.174.

The samples were then sub-divided by using sieves. The sieves used to divide the samples were: 3/4”, 1/2”, 3/8”, No.4, No. 8, No. 16, No. 30, and No. 50. The two coarse aggregate specimens were divided up into the following fractions: passing the 3/4” sieve and retained on the 3/8” sieve, and passing the 3/8” sieve and retained on the No. 4 sieve.

The coarse aggregate specimens had masses of 1000 grams and 330 respectively. As a note, the specimen passing the 3/4” sieve and retained on the 3/8” sieve consisted of two fractions: 700 grams retained on the 1/2” sieve (placed between the 3/4” and 3/8” sieves) and 300 grams retained on the 3/8” sieve. The five fine aggregate specimens were divided up into the following fractions: passing 3/8” and retained on No.4, passing No.4 and retained on No. 8, passing No. 8 and retained on No. 16, passing No. 16 and retained on No. 30, and passing No. 30 and retained on No. 50. Each had a mass of approximately 100 grams.

Next, the specimens were placed into small plastic containers of sodium sulfate solution. The solution provided at least half an inch of cover, and lids were used to close the containers. The specimens were kept in the solution for 16 to 18 hours. Afterwards, the specimens were taken out of the solution and drained for five to ten minutes over a sieve with openings smaller than the designated sieve’s size relative to the specimen. Then, the specimens were placed into the oven at 230 °F and dried to constant mass. Oven-drying the specimens to constant mass took approximately four to six hours. Finally, each specimen was sieved over the designated sieve in order to determine the mass at the end of the cycle.

The process of immersing, draining, oven-drying, and sieving was repeated over a span of five cycles. After the fifth and final cycle was completed, the final masses of the specimens were recorded and used to calculated the Final % Loss. The Final % Loss was

calculated using the equation: $\%Loss = \frac{A-B}{A} x\,100\%$. The initial mass of the specimen is denoted by *A* and the final mass by *B*.

3.3.5 Specific Gravity and Absorption

The specific gravity and absorption test was used to measure the oven-dry specific gravity, saturated-surface-dry specific gravity, apparent specific gravity, and absorption of the aggregate specimens. The sample consisted of particles larger than the No. 8 sieve. Samples were submerged in water for 24 hours so that the samples reached saturation. The sample was removed from the water and an absorbent towel was used to dry the surface of the aggregates so that they were in the saturated-surface-dry condition. The aggregates were then weighed to get the saturated-surface-dry weight (denoted by B). Next, the sample was placed into a wire basket and weighed while submerged in water to obtain the weight of the sample while in water (denoted by C). The sample was then dried to constant mass in the oven at 230 °F and the weight of the dry sample was recorded (denoted by A). The oven-dry specific gravity, G_s (OD), was calculated using equation (3.2). The saturated-surface-dry specific gravity, G_s (SSD), was calculated using equation (3.3), apparent specific gravity, G_s (Apparent), was calculated using equation (3.4). Absorption was calculated using equation (3.5) and is expressed as a percentage.

$$G_s(OD) = \frac{A}{B-C} \tag{3.2}$$

$$G_s(SSD) = \frac{B}{B-C} \tag{3.3}$$

$$G_s(Apparent) = \frac{A}{A - C} \tag{3.4}$$

$$Absorption = \frac{B - A}{A} x100\% \tag{3.5}$$

3.3.6 Standard Compaction Test

The compaction test is used to obtain a relationship between the moisture content and dry unit weight. From the established relationship, the optimum moisture content can be determined. The optimum moisture content occurs at the point where maximum dry density would be achieved, which is the peak of the moisture content-vs-unit weight graph.

The primary instruments used for the standard compaction test were a cylindrical mold with a detachable base-plate and collar, and a mechanical rammer. The cylindrical mold used had an inside diameter of 6” and a height of 4.59”. The rammer had a weight of 5.5 lbf.

A representative sample of the aggregate was obtained. The sample was sieved over a 3/4” sieve and the material retained on the sieve was replaced with material passing the 3/4” sieve and retained on the No. 4 sieve. A specimen was obtained from the sample and an appropriate amount of water was added. The mold and base and the base-plate were weighed while empty. The aggregate specimen was placed into the mold in three layers. Each layer was compacted by raising the rammer up to a height of 12” and allowing it to fall freely. The cycle of the hammer being raised and falling is referred to

as a blow. 56 blows were applied to the layer. Then another layer was added and the same process was repeated. Finally, the third layer was added and compacted in the same manner. The excess aggregate at the top of the mold was trimmed off with a straight edge. The specimen together with the mold and base plate were weighed (as one mass). The weight of the specimen was determined by subtraction the mass of the empty mold and base plate from the mass of the specimen together with the mold and base plate. The volume of the specimen was determined by using the dimensions of the mold and the formula for the volume of a cylinder. The moist unit weight of the compacted specimen was calculated by dividing the weight of the specimen by its volume.

Additionally, a sub-specimen was obtained from the specimen. The sub-specimen was placed into a container and weighed. This sub- specimen, while in the container, was dried to constant mass and the mass was recorded afterwards as well. The mass of the water contained in the sub-specimen was determined by subtracting its dry mass from its moist mass. The moisture content of the specimen was determined by dividing the mass of water by the dry mass of the sub-specimen. The dry unit weight of the specimen was calculated by using the equation:

$$\gamma_d = \frac{\gamma_m}{1+\omega} \tag{3.6}$$

In equation (3.6), γ_d is the dry unit weight, γ_m, is the moist unit weight, and ω is the moisture content.

On average, approximately five specimens with different moistures contents were compacted so that there were enough points on the compaction curve for determining the

optimum moisture content. The moisture content is the point corresponding to the maximum dry unit weight on the compaction curve. Visually, the maximum dry unit weight is the peak of the compaction curve.

3.3.7 California Bearing Ratio

The California Bearing Ratio test is one way of evaluating the strength of base course aggregates. The equipment used for the CBR test included a CBR mold, perforated base plate, spacer disk, filter paper, a large container of water, and a loading machine. Samples of base-course aggregate was prepared in a similar manner as they were for the standard compaction test. As was done for compaction, the sample was sieved over a 3/4” sieve and the material retained on the sieve was replaced with material passing the 3/4” sieve and retained on the No. 4 sieve. The sample was prepared at optimum moisture content.

The CBR mold (with an inside diameter of 6” and a height of 7”) was weighed and the mass was recorded. The spacer disk (with a dimeter and height of) was placed onto the base plate and the CBR mold was placed over it. A sheet of filter paper was placed on the spacer disk. Then, the sample was prepared in the same manner as it was for compaction except that 76 blows were applied to each layer. After compaction, the mold and the sample were weighed together. The mold with the sample inside was then flipped upside down and placed back onto the base plate. Two surcharge weights weighing 10 lbs in total were placed on top of the specimen. Then the sample was fully submerged in a container of water for 96 hours so that the sample would be tested while

it was in its weakest condition. After 96 hours passed, the sample was removed from the water container. The free water on the top was removed and the sample was allowed to drain for at least 15 minutes.

Afterwards, the sample was placed onto the loading machine and a piston was attached to the load frame. Bluehill software was used to run the test. The piston was lowered through the circular hole in the surcharge weights and seated onto the top of the specimen. The load was then applied at a rate of 0.05 inches per minute and the load values were recorded by the software ensuring that the load values at the necessary penetration depths were obtained.

After the load and penetration data were collected, the load was divided by the cross-sectional area of the piston (3 in^2) to calculate the stress on the piston. The penetration depth was plotted against the stress to get the curve that was needed to determine the CBR value. The first step of determining the CBR value was to make a correction to the CBR curve if necessary. The correction was made by drawing a line over the linear portion of the CBR curve until it hit the x-axis (penetration). The x-intercept was used as a reference point. For the penetration located at 0.1 inches from the reference point, the corresponding stress was determined. Once the stress was determined, the CBR value (expressed in terms of percent) was calculated by dividing the stress determined at 0.1 inches from the reference point by the standard stress of 1000 psi and multiplying that value by 100.

3.4 Regression Analysis

Correlation and regression provide measures such as the correlation coefficient (r), coefficient of determination (R^2), and regression equations used as mathematical prediction models. The correlation coefficient measures the strength of a relationship between two variables, and the coefficient of determination is a measure that explains the percentage of variation in one variable that can be explained by the regression equation (Bluman 2004).

Regression analyses were employed to assess the performance-quality of the aggregate samples collected for the study. The regression line separates the aggregates with good performance from the aggregates with poor performance. An aggregate below the regression line indicates good performance and an aggregate directly (vertically) above that aggregate does not have as good a performance-quality. An aggregate on the regression line is not considered to have either good or poor performance. An aggregate above the regression line indicates that it has poor performance.

The regression analyses compared mass loss of coarse aggregates by Micro-Deval abrasion versus coarse aggregate absorption, mass loss of coarse aggregates by sodium sulfate soundness versus absorption, and mass loss of coarse aggregates by sodium sulfate soundness versus mass loss of coarse aggregates by Micro-Deval abrasion for nine different sets of data. The data sets were obtained from “Testing Methods to Determine Long Term Durability of Wisconsin Aggregate Resources” which is referred to as WHRP-1 (Weyers et al., 2005), “Investigation of Testing Methods to Determine Long-

Term Durability of Wisconsin Aggregates" which is referred to as WHRP-2 (Tabatabai et al., 2013), a data set from Omni which is referred to as WHRP-3 (2017), and the samples collected for this study which is referred to as Current Study.

The nine data sets that were used for regression analyses were 1) All virgin aggregates from WHRP-1; 2) Virgin aggregates with good performance from WHRP-1; 3) Virgin aggregates with intermediate performance from WHRP-1; 4) Virgin aggregates with poor performance from WHRP-1; 5) Virgin aggregates with poor performance from WHRP-2; 6) Virgin aggregates with mixed, yet unknown, performance from WHRP-3; 7) Aggregates with mixed performance from the current study; 8) All virgin aggregates from WHRP-1, WHRP-2, and WHRP-4; and 9) All aggregates from all studies.

The regression models and coefficients of determination were identified and organized into a table to compare in order to select a regression model that could be used as a basis to accurately determine the performance quality of aggregates.

After a regression model was chosen, the points from the current study alone were placed on the same graph as the regression model to compare their position relative to the regression line. The points above the regression line indicate that aggregates had good performance and the points located below indicate that aggregates had poor performance.

The strategy in addressing the research investigation by using regression analysis was to respond to the following tasks: 1) Evaluate the properties of base-course

aggregates used in roadway construction over the time elapsed; 2) Explore various regression models; 3) Establish criteria for making the selection of the most suitable regression model; 4) Set criteria to identify which aggregates indicate good performance and which aggregates indicate potential poor performance by using the selected regression model; and 5) Use the selected regression model to assess the performance quality of aggregates that served in base-course layers.

3.5 Comparison with Threshold Limits

The results of the mass loss of coarse aggregates by Micro-Deval abrasion, mass loss of coarse aggregates by sodium sulfate soundness, and coarse aggregate absorption were displayed by bar graphs. Threshold limits were selected in order to compare the test results with them. The threshold limits were selected based on WisDOT specifications and recommend limits from other sources. For Micro-Deval abrasion, a threshold limit of 18% was selected based on the recommendation made by Kandhal and Parker (1998). For sodium sulfate soundness, a threshold limit of 18% was selected based on the WisDOT specifications. For absorption, a threshold limit of 2% was selected based on recommendation made by Pigeon and Pleau (1995). Horizontal lines representing specified threshold limits were added on to the bar graphs to determine which aggregate samples collected for this study exceeded the threshold limit and which ones did not.

CHAPTER 4

RESULTS

This chapter presents the results obtained from the various lab tests that were conducted for this research. The results include the grain-size distributions, mass loss by Micro-Deval abrasion, mass loss by sodium sulfate soundness, specific gravity, absorption, optimum moisture content and maximum dry density, CBR values, and DCP results.

4.1 Grain-Size Distribution

The graph in Figure 4.1 shows the grain-size distribution of each sample and where each one falls relative to the lower limit and upper limit in accordance with the aggregate base layer specifications established by WisDOT (FDM, 2017). The graph shows that the grain-size distributions of the samples mostly fell within the standard limits, but partly escaped the top boundary. As a note, sieve analysis was not performed on Jefferson SH-18 because there was not a sufficient quantity to run the test on. However, the grain-size distribution of Jefferson SH-18 was assumed to be the average of the limits on the basis of prior knowledge that the sample complied with the standards. One of the uses of the grain-size distribution is that it is needed to make calculations for the sodium sulfate soundness test. Because of this, an assumed grain-size distribution was made for Jefferson SH-18 in order to get an idea of the sodium sulfate soundness results for it.

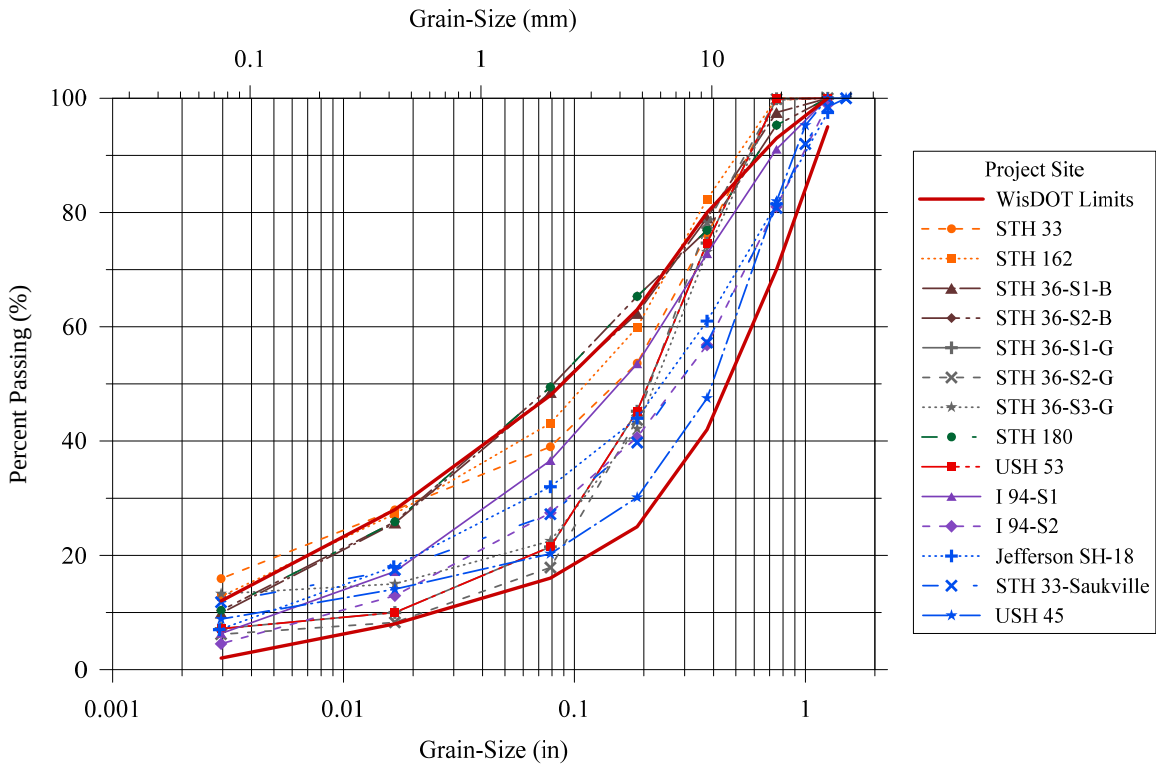

Figure 4.1: Grain-Size Distributions of all samples relative to the standard limits established by WisDOT.

4.2 Micro-Deval Abrasion

The mass loss (expressed as a percentage) by Micro-Deval abrasion of all samples that were collected for this study are summarized in Table 4.1 and displayed as bar graphs in Figures 4.2 (a), 4.2 (b), 4.2 (c).

Table 4.1: Mass Loss of coarse and fine aggregates by Micro-Deval.

Project Site	Mass Loss (%)	
	Coarse	Fine
STH 33	18.7	21.5
STH 162	15.1	18.2
STH 36-S1-B	8.4	16.5
STH 36-S2-B	14.2	16.4
STH 36-S1-G	13.3	24.5
STH 36-S2-G	14.6	25.4
STH 36-S3-G	13.5	25.4
STH 180	18.9	25.7
USH 53	13.9	6.9
I 94-S1	17.2	12.8
I 94-S2	17.5	12.9
Jefferson SH-18	13.0	19.4
STH 33-Saukville	12.0	29.7
USH 45	16.3	28.5

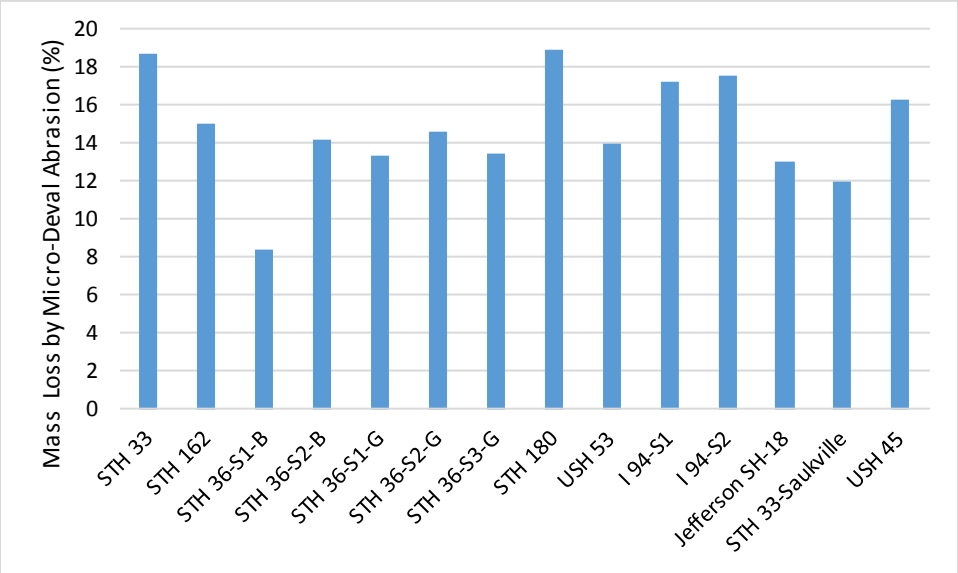

Figure 4.2 (a): Mass loss of coarse aggregate due to the Micro-Deval test.

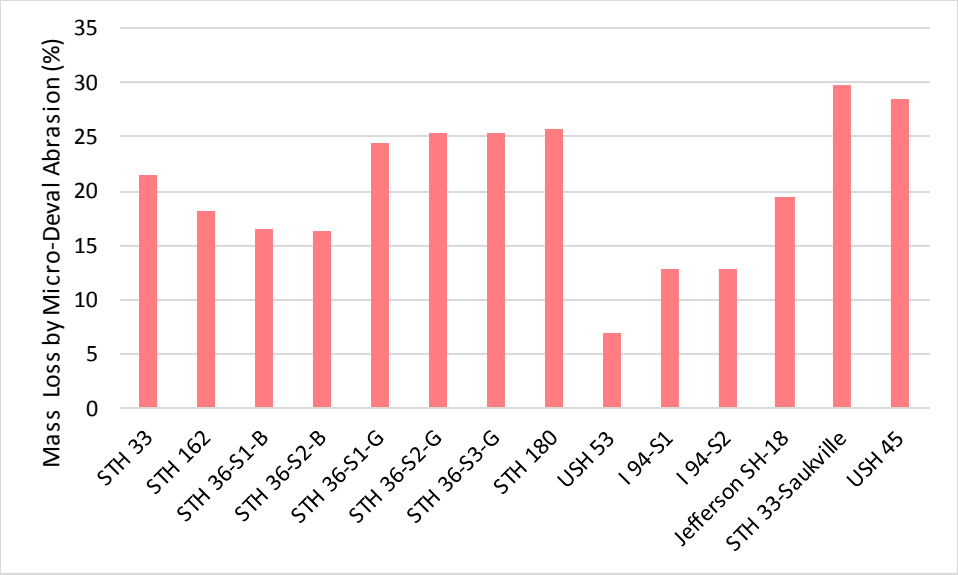

Figure 4.2 (b): Mass loss of fine aggregate due to the Micro-Deval test.

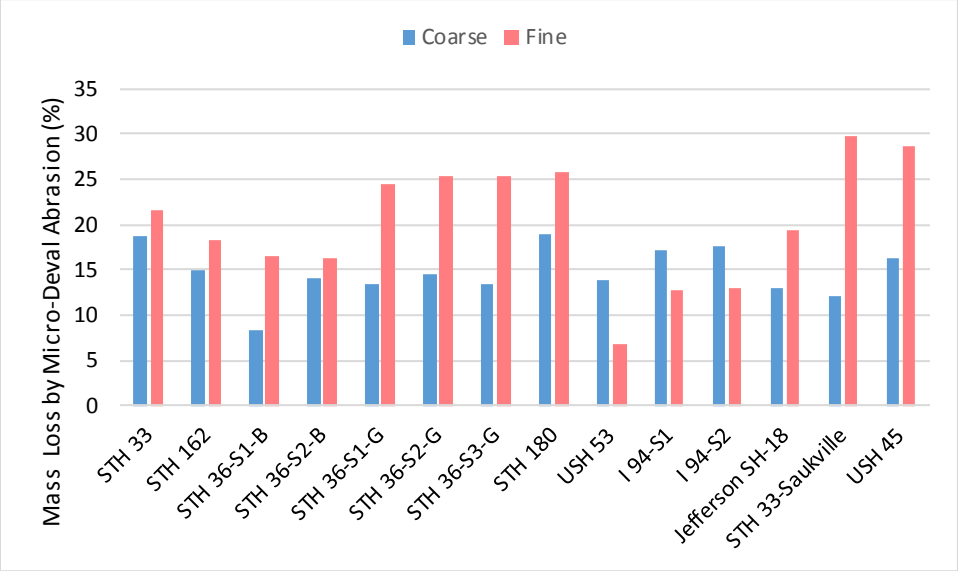

Figure 4.2 (c): Mass loss of coarse and fine aggregate due to the Micro-Deval test.

As can be seen in the table and bar graphs, the mass losses for coarse aggregates ranged from 8.4% (STH 36-S1-B) to 18.9% (STH 180). Note that these two samples are aggregates from existing base-course layers. For fine aggregates, the mass losses ranged from 6.9% (USH 53) to 29.7% (STH 33-Saukville). Note that STH 33-Saukville was a

newly placed virgin aggregate. Limiting the range to aggregates from existing base-course layers only, the mass losses for fine aggregates ranged from 6.9% (USH 53) to 25.7% (STH 180). As can be seen in Figure 4.2 (c), fine aggregates generally had greater mass losses by Micro-Deval abrasion when compared with coarse aggregates except for USH 53, I 94-S1, and I 94-S2.

4.3 Sodium Sulfate Soundness

The mass loss (expressed as a percentage) by sodium sulfate soundness of all samples that were collected for this study are summarized in Table 4.2 and displayed as bar graphs in Figures 4.3 (a), 4.3 (b), 4.3 (c).

Table 4.2: Mass Loss of coarse and fine aggregates by sodium sulfate.

Project Site	Mass Loss (%)	
	Coarse	Fine
STH 33	7.7	13.7
STH 162	1.4	4.1
STH 36-S1-B	6.6	10.8
STH 36-S2-B	3.5	4.4
STH 36-S1-G	3.3	7.0
STH 36-S2-G	2.4	8.2
STH 36-S3-G	3.1	7.2
STH 180	5.5	7.2
USH 53	3.9	5.3
I 94-S1	16.6	10.9
I 94-S2	13.8	9.2
Jefferson SH-18	1.5	7.6
STH 33-Saukville	0.8	2.6
USH 45	4.2	5.6

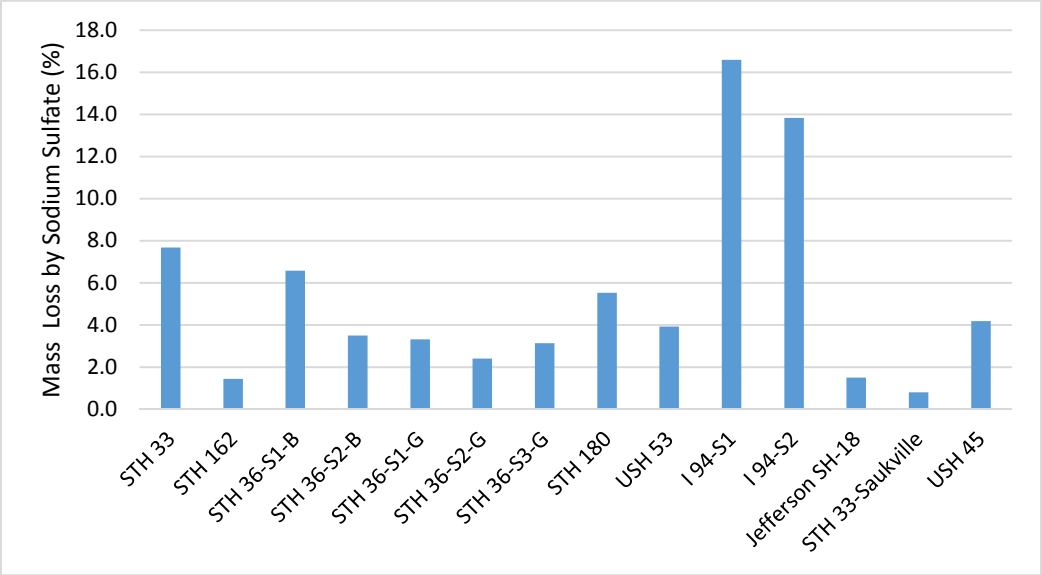

Figure 4.3 (a): Final mass loss of coarse aggregate due to the sodium sulfate soundness test.

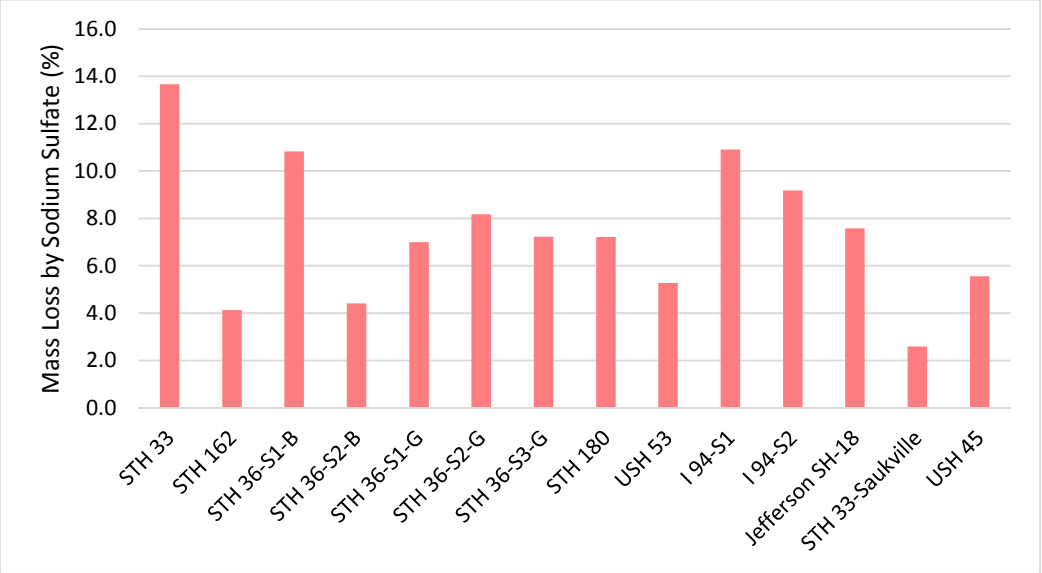

Figure 4.3 (b): Final mass loss of fine aggregate due to the sodium sulfate soundness test.

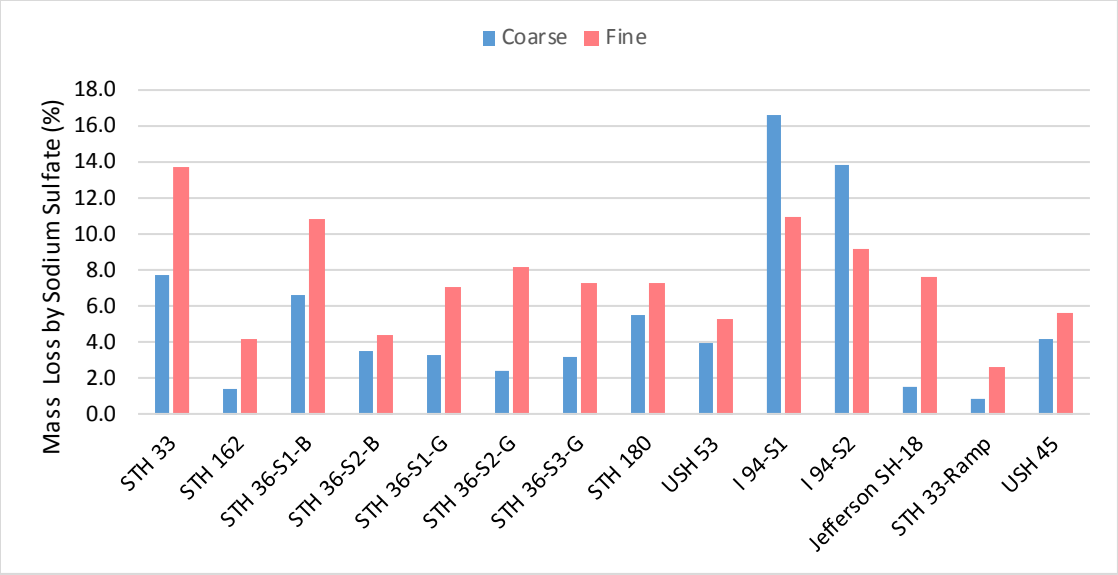

Figure 4.3 (c): Final mass loss of coarse and fine aggregate due to the sodium sulfate soundness test.

As can be seen in the table and bar graphs, the mass losses for coarse aggregates ranged from 0.8% (STH 33-Saukville) to 16.6% (I 94-S1). Note that STH 33-Saukville was a newly placed virgin aggregate. Limiting the range to aggregates from existing base-course layers only, the mass losses for coarse aggregates ranged from 1.4 % (STH 162) to 16.6% (I 94-S1).

For fine aggregates, the mass losses ranged from 2.6% (STH-Saukville) to 13.7% (STH 33). As noted earlier, STH 33-Saukville was a newly placed virgin aggregate. Limiting the range to aggregates from existing base-course layers only, the mass losses for fine aggregates ranged from 4.1% (STH 162) to 13.7% (STH 33). As can be seen in Figure 4.3 (c), fine aggregates generally had greater mass losses by sodium sulfate soundness when compared with coarse aggregates except for I 94-S1 and I 94-S2.

For sodium sulfate soundness, the cumulative mass loss was also determined after each cycle for each specimen for coarse aggregates. For fine aggregates, the cumulative mass loss after each cycle was only determined for the following specimens: STH 33, STH 162, STH 36-S1-B, STH 180, USH 53, I 94-S1, and I 94-S2. The cumulative mass loss per cycle for coarse aggregates is displayed in Figure 4.4 (a), and the cumulative mass loss per cycle for fine aggregates is displayed in Figure 4.4 (b).

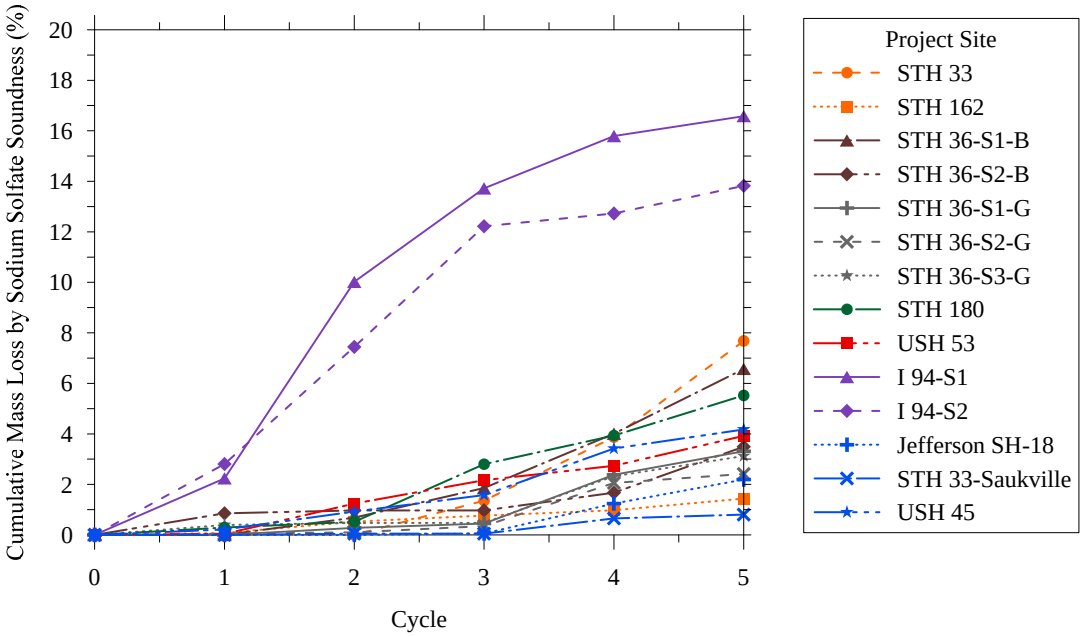

Figure 4.4 (a): Cumulative mass loss of coarse aggregates by sodium sulfate soundness per cycle.

For coarse aggregates, the highest rate of mass loss occurred between Cycle 1-to-2 for the following two samples: STH 162 and USH 53. The highest rate of mass loss occurred between Cycle 2-to-3 for the following two samples: I 94-S1 and I 94-S2. The highest rate of mass loss occurred between Cycle 3-to-4 for the following six samples: STH 36-S1-G, STH 36-S2-G, STH 36-S3-G, Jefferson SH-18, STH 33-Saukville, and

USH 45. The highest rate of mass loss occurred between Cycle 4-to-5 for the following six samples: STH 33, STH 162, STH 36-S1-B, STH 36-S2-B, STH 180, and USH 53. Note that STH 162 and USH 53 experienced their highest rate of mass loss in both Cycle 1-to-2 and Cycle 4-to-5. It is also worth noting that there seemed to be a trend where the highest rate of mass loss occurred either between Cycle 3-to-4 or Cycle 4-to-5 for most samples.

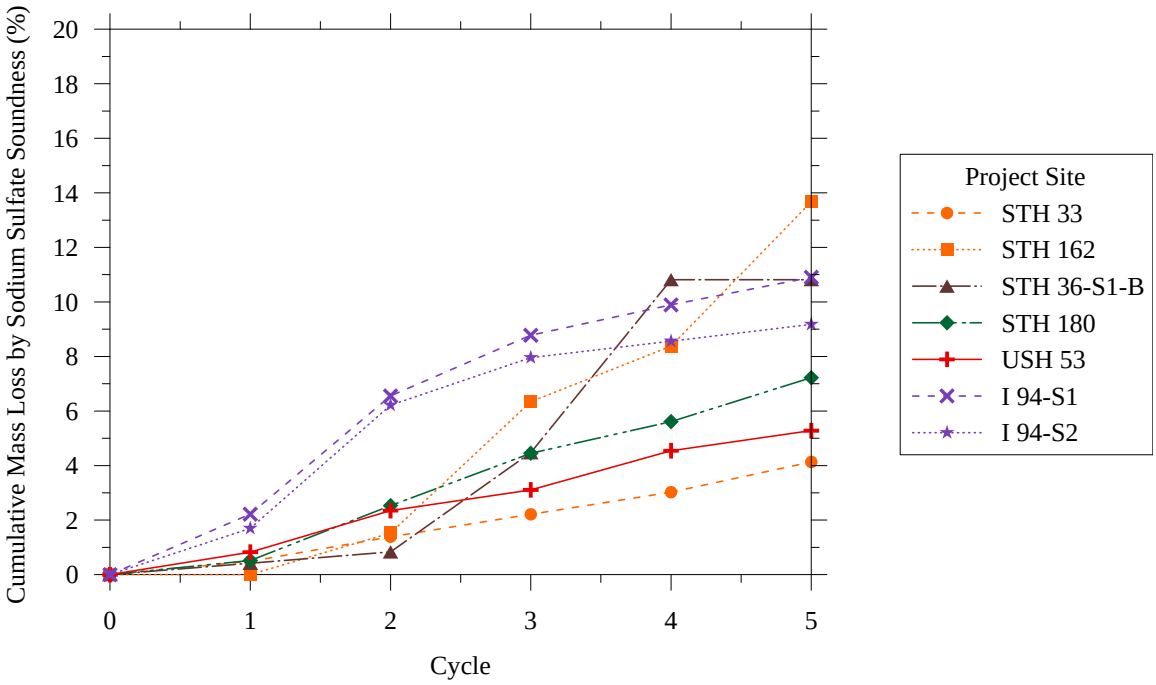

Figure 4.4 (b): Cumulative mass loss of fine aggregates by sodium sulfate soundness per cycle.

For fine aggregates, the highest rate of mass loss occurred between Cycle 1-to-2 for the following four samples: STH 180, USH 53, I 94-S1, and I 94-S2. The highest rate of mass loss occurred between Cycle 2-to-3 for STH 180. Note that for STH 180, the rate of mass loss was the same from Cycle 1-to-2 and Cycle 2-to-3. The highest rate of mass

loss occurred between Cycle 3-to-4 for STH 36-S1-B. The highest rate of mass loss occurred between Cycle 4-to-5 for STH 33 and STH 162.

4.4 Specific Gravity

The oven-dry (OD) specific gravity, saturated-surface dry (SSD), and apparent specific gravity of all samples that were collected for this study are summarized in Table 4.3 and displayed in Figures 4.5 (a), 4.5 (b), and 4.5 (c).

Table 4.3: Oven-dry, saturated-surface-dry, and apparent specific gravity for each sample.

Project Site	Specific Gravity		
	OD	SSD	Apparent
STH 33	2.60	2.67	2.79
STH 162	2.63	2.68	2.75
STH 36-S1-B	2.64	2.70	2.80
STH 36-S2-B	2.64	2.69	2.79
STH 36-S1-G	2.66	2.71	2.81
STH 36-S2-G	2.62	2.68	2.78
STH 36-S3-G	2.64	2.70	2.81
STH 180	2.67	2.70	2.76
USH 53	2.65	2.70	2.78
I 94-S1	2.38	2.47	2.63
I 94-S2	2.42	2.51	2.66
Jefferson SH-18	2.59	2.66	2.79
STH 33-Saukville	2.63	2.68	2.77
USH 45	2.73	2.76	2.82

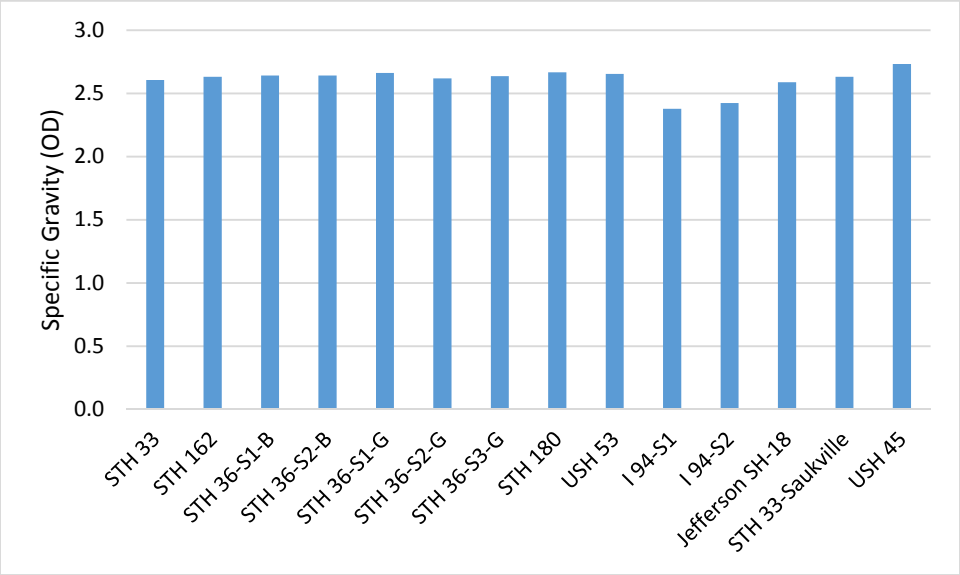

Figure 4.5 (a): Oven-dry specific gravity of coarse aggregates.

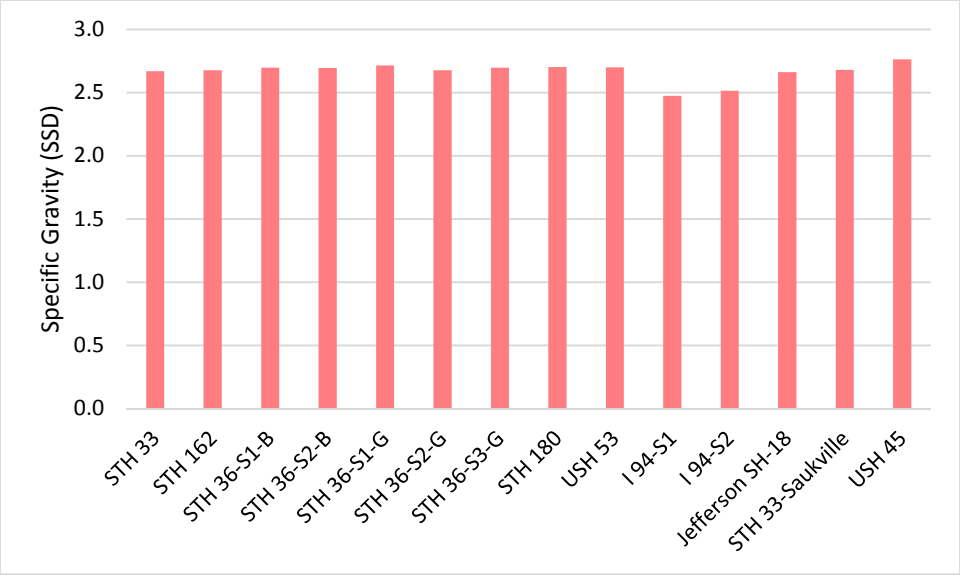

Figure 4.5 (b): Saturated-surface-dry specific gravity of coarse aggregates.

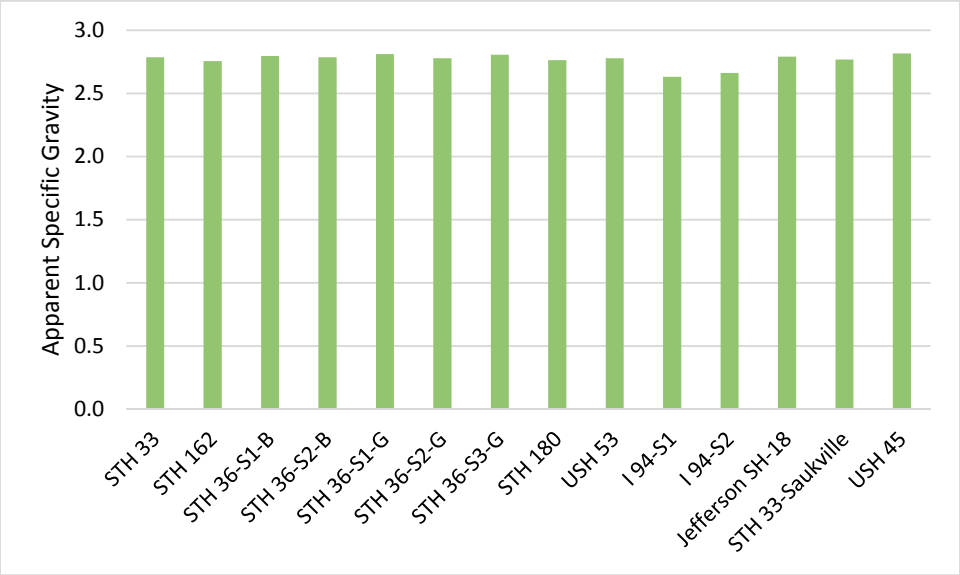

Figure 4.5 (c): Apparent specific gravity of coarse aggregates.

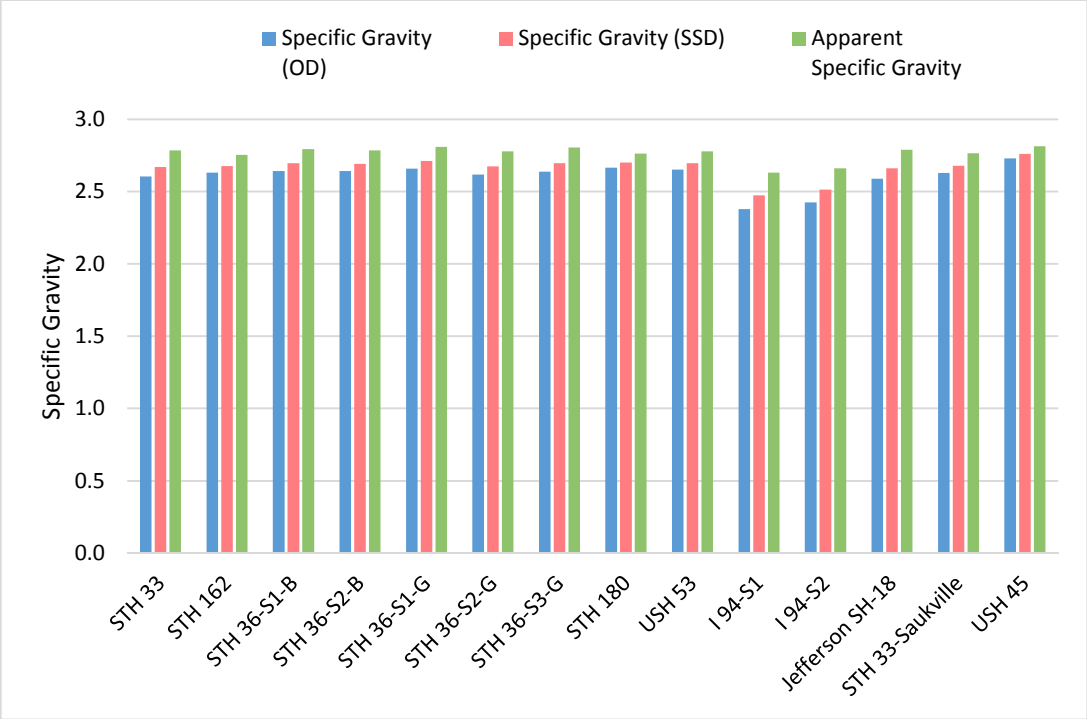

Figure 4.5 (d): Oven-dry, saturated-surface-dry, and apparent specific gravity.

For oven-dry specific gravity, values ranged from 2.38 (I 94-S1) to 2.73 (USH 45). Note that USH 45 is a virgin aggregate. Limiting the range to aggregates from existing base-course layers only, the oven-dry specific gravity ranged from 2.38 (I 94-S1) to 2.67 (STH 180). For saturated-surface-dry specific gravity, values ranged from 2.47 to 2.76. Limiting the range to aggregates from existing base-course layers only, the saturated-surface-dry specific gravity ranged from 2.47 (I 94-S1) to 2.71 (STH 36-S1-G). For apparent specific gravity, values ranged from 2.63 (I 94-S1) to 2.82 (USH 45). Limiting the range to aggregates from existing base-course layers only, the apparent specific gravity ranged from 2.63 (I 94-S1) to 2.81 (STH 36-S1-G and STH 36-S3-G).

4.5 Absorption

The absorption values of all samples that were collected for this study are summarized in Table 4.4 and displayed in Figure 4.6. The absorption values ranged from 1.09% (USH 45) to 4.05% (I 94-S1). Limiting the range to aggregates from existing base-course layers only, the absorption ranged from 1.30 (STH 180) to 4.05 (I 94-S1).

Table 4.4: Absorption of all samples.

Project Site	Absorption (%)
STH 33	2.50
STH 162	1.70
STH 36-S1-B	2.08
STH 36-S2-B	1.97
STH 36-S1-G	2.00
STH 36-S2-G	2.20
STH 36-S3-G	2.28
STH 180	1.30
USH 53	1.70
I 94-S1	4.05
I 94-S2	3.66
Jefferson SH-18	2.78
STH 33-Saukville	1.89
USH 45	1.09

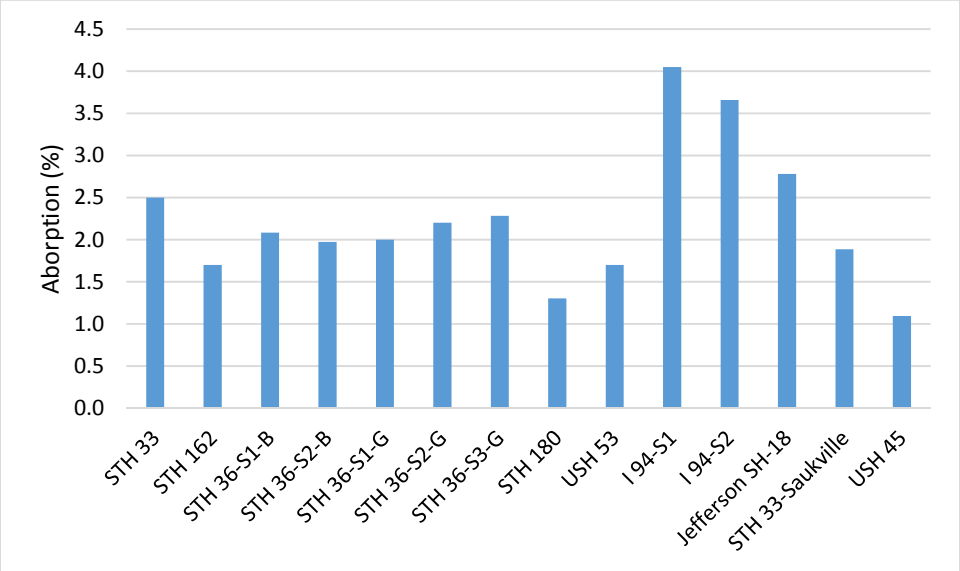

Figure 4.6: Absorption of coarse aggregates.

4.6 Compaction

The compaction curves are displayed in Figure 4.7, and a summary of the optimum moisture content and maximum dry density values is given in Table 4.5.

The moisture content values ranged from 3.64% (STH 180) to 8.05% (I 94-S1) with corresponding maximum dry unit weight values of 134.96 lb/ft^3 and 131.55 lb/ft^3 respectively. Note that this range of these two values are for aggregates from existing base-course layers, while the newly placed virgin aggregates are also included within this range. Additionally, the maximum dry unit weight values ranged from 131.55 lb/ft^3 (I 94-S1) to 149.20 lb/ft^3 (USH 45). Limiting the range to aggregates from existing base-course layers, the values ranged from 131.55 lb/ft^3 to 147.36 lb/ft^3.

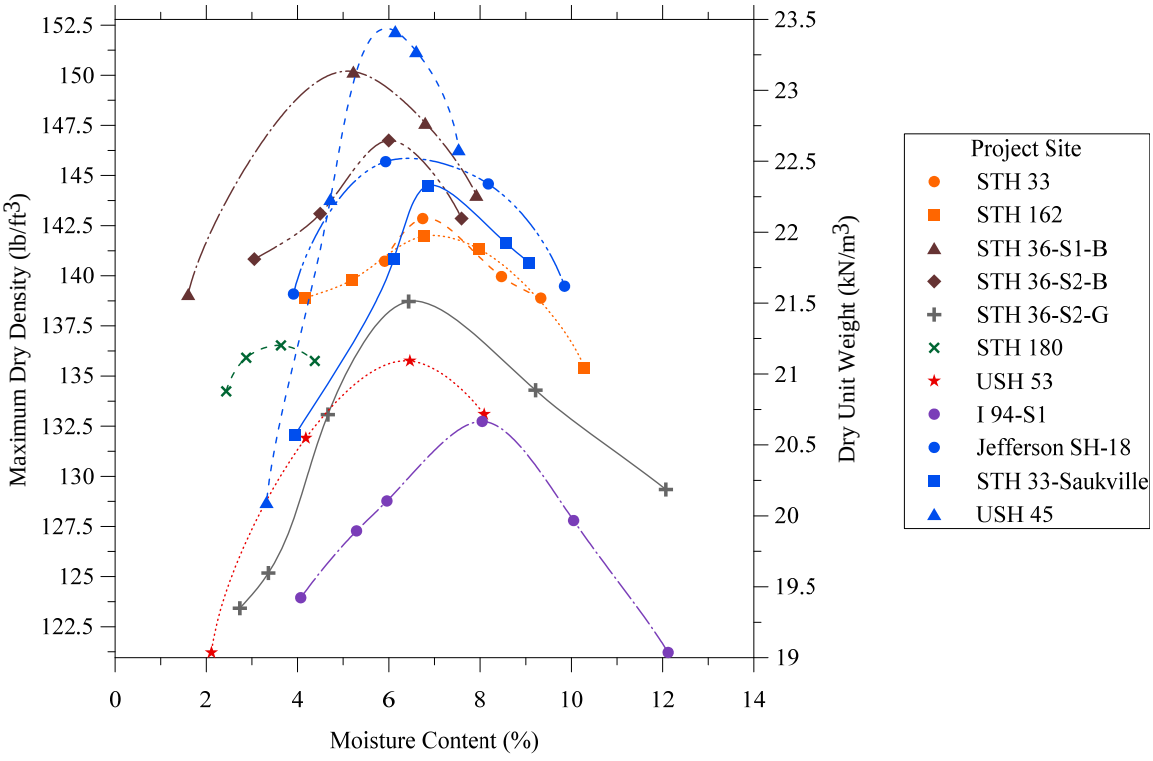

Figure 4.7: Compaction curves of all samples.

Table 4.5: Maximum dry unit weight ($\gamma_{d,max}$) and optimum moisture content (ω_{opt}) of each sample.

Project Site	$\gamma_{d,max}$		ω_{opt}
	(lb/ft^3)	(kN/m^3)	(%)
STH 33	140.65	22.10	6.74
STH 162	139.86	21.97	6.77
STH 36-S1-B	147.36	23.15	5.00
STH 36-S2-B	144.15	22.65	6.00
STH 36-S2-G	136.92	21.51	6.43
STH 180	134.96	21.20	3.64
USH 53	134.31	21.10	6.40
I 94-S1	131.55	20.67	8.05
Jefferson SH-18	142.27	22.35	6.50
STH 33-Saukville	142.12	22.33	6.85
USH 45	149.20	23.44	6.30

4.7 California Bearing Ratio

The penetration versus stress curves that were developed from the soaked CBR test are displayed in Figure 4.8, and a summary of the CBR values that were calculated from the graph are displayed in Table 4.6. The samples were prepared at optimum moisture content. It is important to note that optimum moisture contents of aggregates from similar sites were used for samples without available compaction data that consisted of the same type of aggregate. The optimum moisture content of STH 36-S2 G was used for or STH 36-S1G and STH 36-S3-G. The optimum moisture content of I 94-S1 was used for I 94-S2. The CBR values ranged from 43.5% (USH 53) to 89.9 % (STH 36-S3-G).

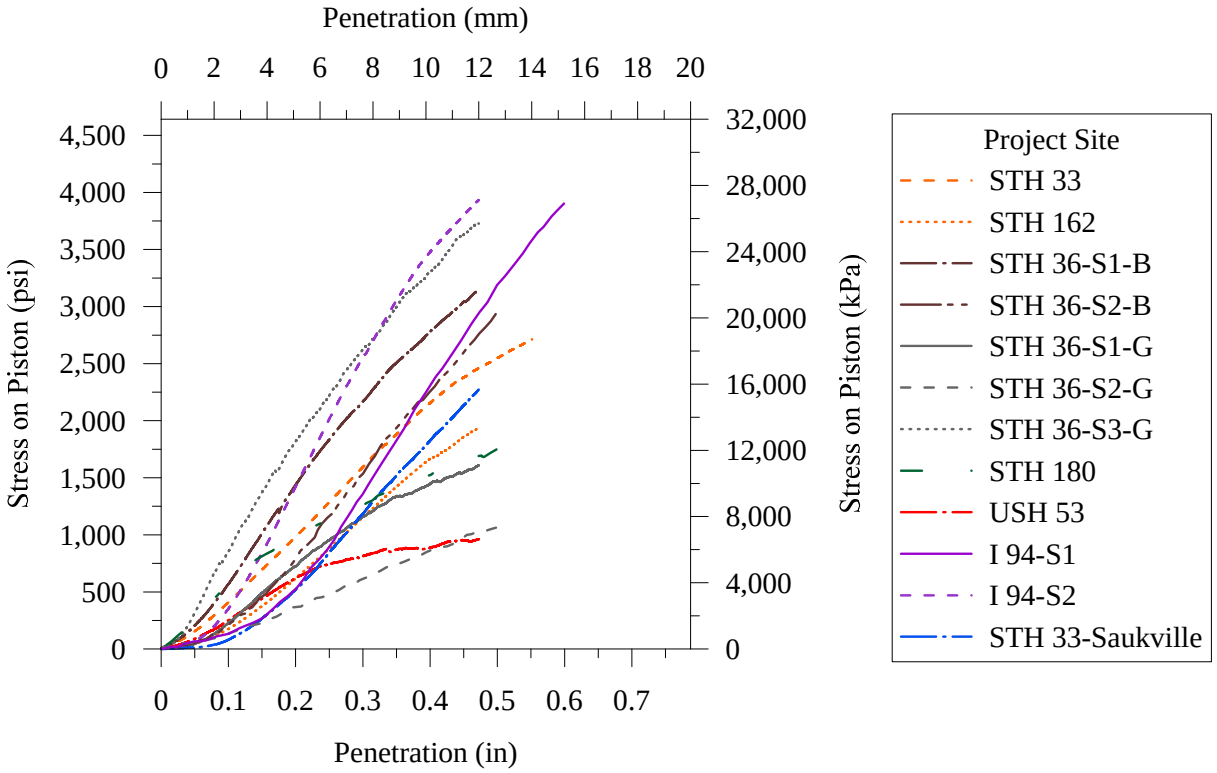

Figure 4.8: Graph of Penetration vs Stress values calculated from the results of the CBR test.

Table 4.6: CBR values calculated from the penetration vs stress graph.

Project Site	CBR (%)
STH 33	58.0
STH 162	55.1
STH 36-S1-B	87.0
STH 36-S2-B	70.0
STH 36-S1-G	53.6
STH 36-S2-G	NA
STH 36-S3-G	89.9
STH 180	56.7
USH 53	43.5
I 94-S1	76.7
I 94-S2	73.9
Jefferson SH-18	NA
STH 33-Saukville	52.2
USH 45	NA

4.8 Dynamic Cone Penetration

The penetration depth and blow counts were used to calculate the penetration rate for each corresponding depth. The penetration rate versus depth graphs obtained from the DCP data are shown in Figure 4.9 (a) through Figure 4.9 (g).

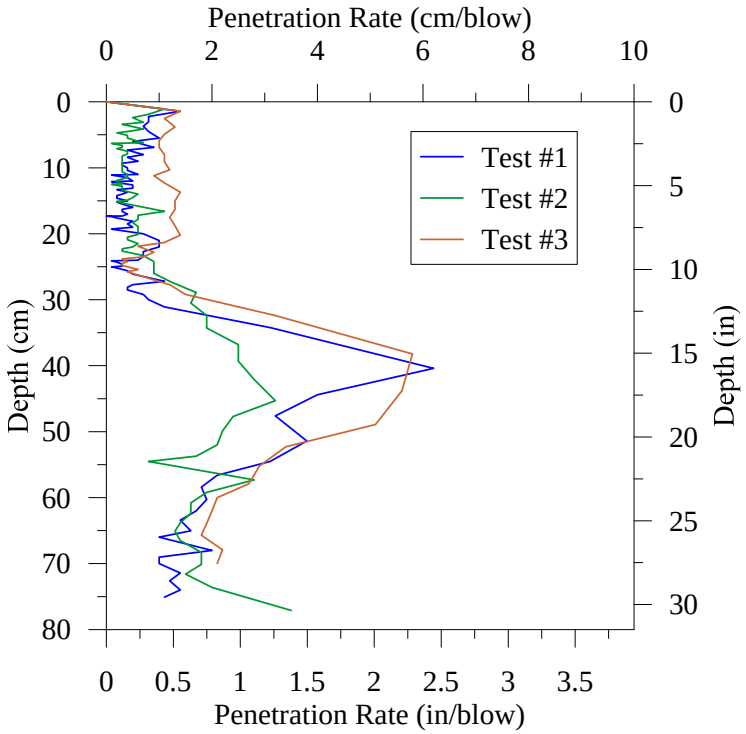

Figure 4.9 (a): Graph of penetration rate vs depth for STH 33.

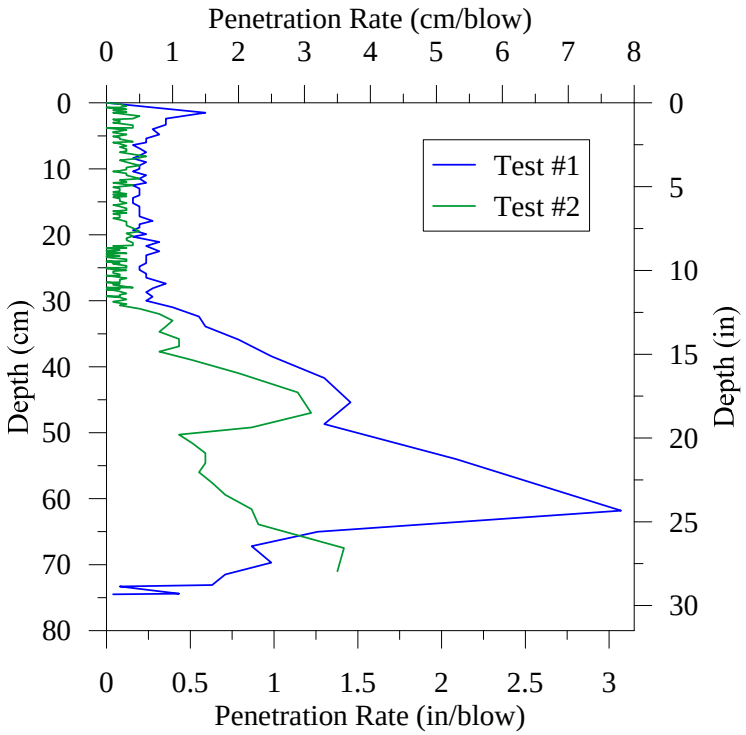

Figure 4.9 (b): Graph of penetration rate vs depth for STH 162.

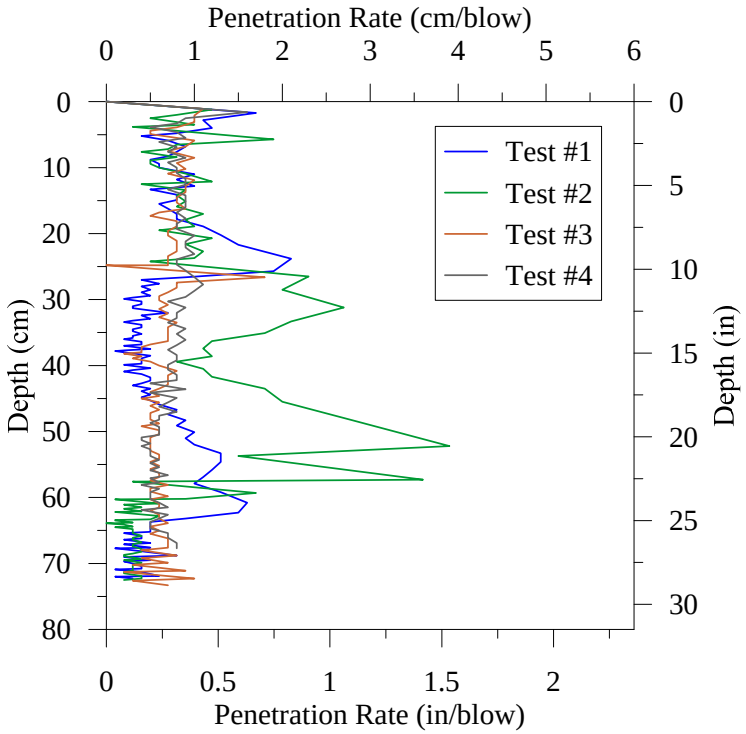

Figure 4.9 (c): Graph of penetration rate vs depth for STH 36-S1.

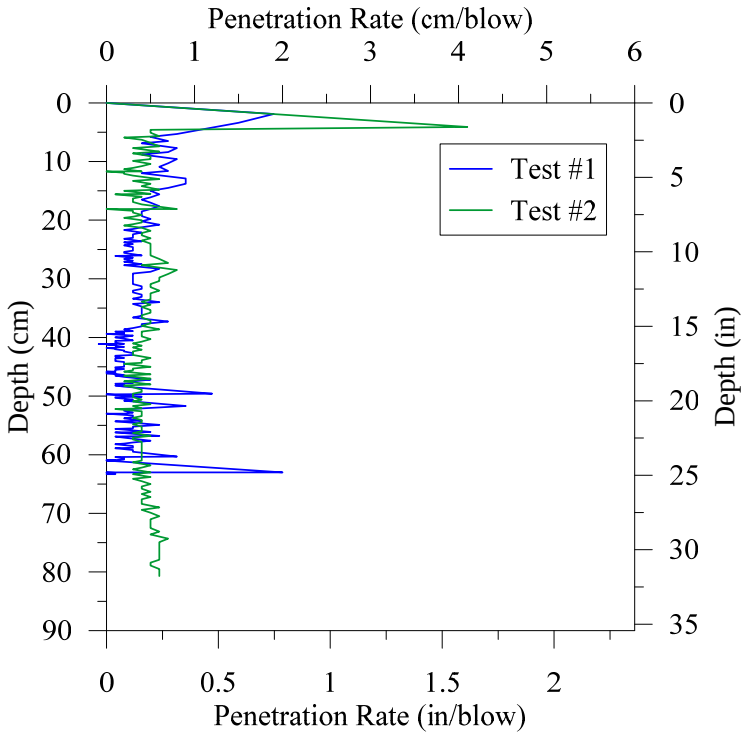

Figure 4.9 (d): Graph of penetration rate vs depth for STH 36-S2.

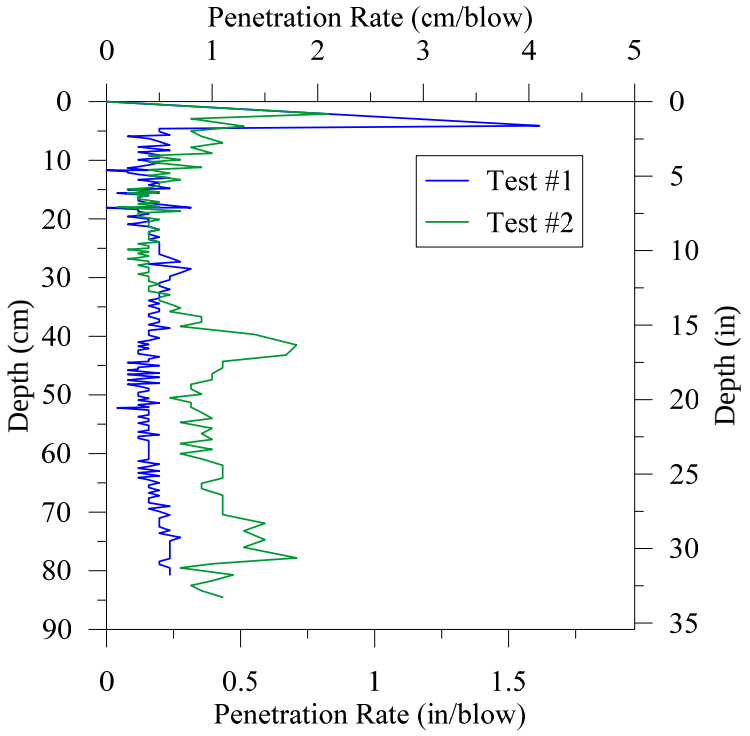

Figure 4.9 (e): Graph of penetration rate vs depth for STH 36-S3.

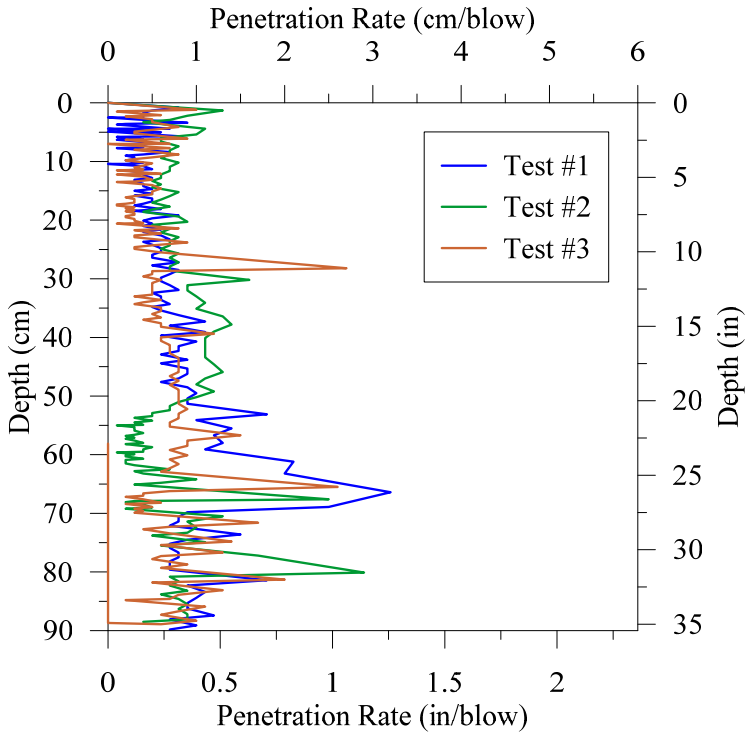

Figure 4.9 (f): Graph of penetration rate vs depth for STH 180.

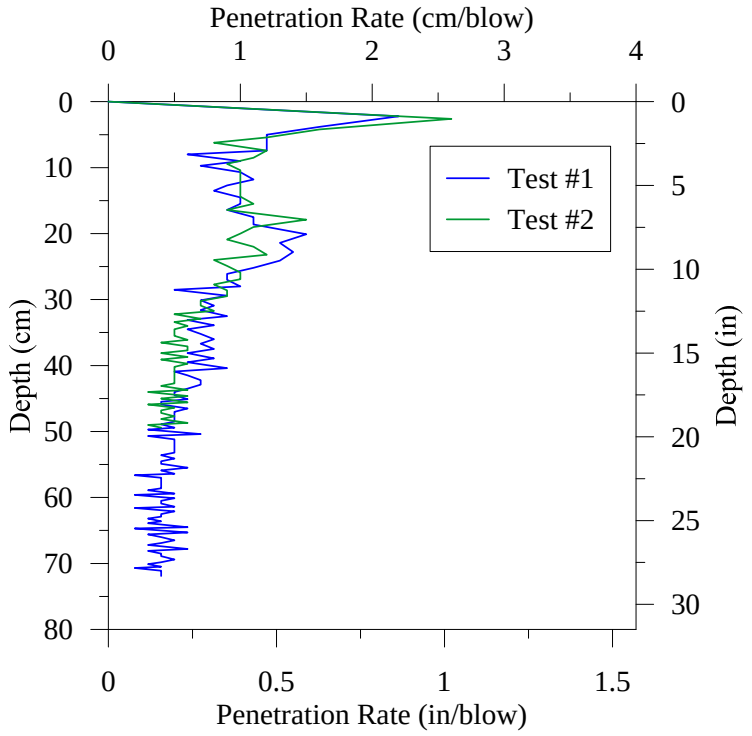

Figure 4.9 (g): Graph of penetration rate vs depth for USH 53.

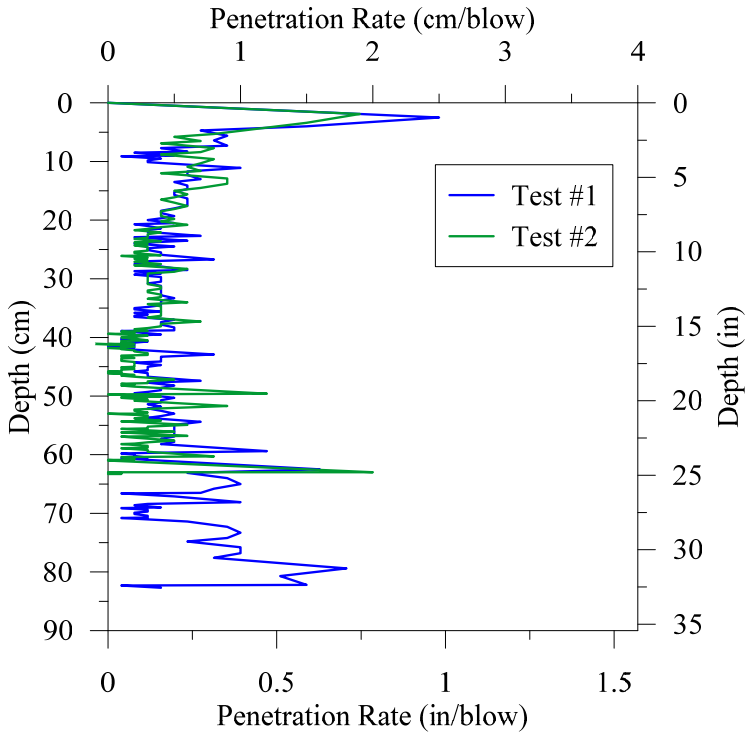

Figure 4.9 (h): Graph of penetration rate vs depth for I 94-S2.

CHAPTER 5

ANALYSIS OF TEST RESULTS

This chapter presents a detailed analysis of the results summarized in Chapter 4. For the analysis of the Micro-Deval abrasion, sodium sulfate soundness, and absorption data, only coarse aggregates were taken into account. Regression analyses were performed on the Micro-Deval abrasion, sodium sulfate soundness, and aggregate absorption data collected for this study in combination with data obtained from other sources. Bar graphs coupled with horizontal lines representing WisDOT and recommended threshold limits were produced from the Micro-Deval abrasion, sodium sulfate soundness and aggregate absorption data collected for this study.

For the comparison of mass loss by Micro-Deval abrasion versus absorption, all the graphs along with a summary table displaying the regression equations and coefficients of determination are presented. For the comparison of mass loss by sodium sulfate soundness versus absorption and the comparison of Micro-Deval abrasion versus sodium sulfate soundness, only summary tables along with the graphs of the regression analyses that considered all data points combined are presented. Displaying the other graphs was not necessary because the Micro-Deval versus absorption regression analyses that showed strong correlations indicated stronger correlations yet than those performed on sodium sulfate versus absorption and those performed on sodium sulfate versus Micro-Deval. Additionally, the average CBR values that were estimated from the DCP test results were compared with the soaked CBR values determined from the CBR test.

5.1 Comparison with Threshold Limits

The bar graphs below present the results of the Micro-Deval abrasion, sodium sulfate soundness, and aggregate absorption tests specific to the samples that were collected for this study. Each bar graph is accompanied with a horizontal line that represents a specified threshold limit. The threshold limit used for mass loss by Micro-Deval abrasion was a recommended value of 18%. The threshold limit used for mass loss by sodium sulfate soundness was the WisDOT limit of 18%. The threshold limit used for absorption was a recommended value of 2%.

The bar graph in Figure 5.1 shows the mass loss of coarse aggregates by Micro-Deval abrasion. The mass loss values were compared with the threshold limit of 18%. All mass loss values fell below the limit with the exception of STH 33 and STH 180. As can be seen in the figure, two out of the fourteen samples collected exceeded the recommended threshold limit. Note that the two samples that exceeded the recommended threshold limit were from existing base-course layers. Therefore, two out of the eleven aggregates from existing base-course layers exceeded the recommended threshold limit.

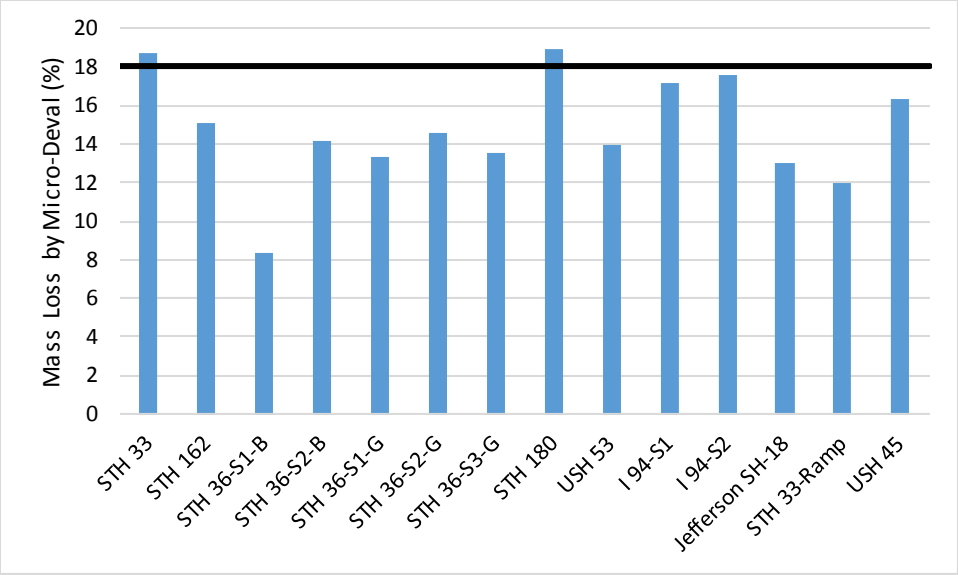

Figure 5.1: Bar graph displaying the results of the mass loss of coarse aggregates by Micro-Deval abrasion and showing the recommended threshold of 18%.

The bar graph in Figure 5.2 shows the mass loss of coarse aggregates by sodium sulfate soundness. The mass loss values were compared with the recommended threshold limit of 18%. All mass loss values fell below the limit. Thus, none of aggregates from existing base-course aggregate layers and none of the virgin aggregates exceeded the recommended threshold limit.

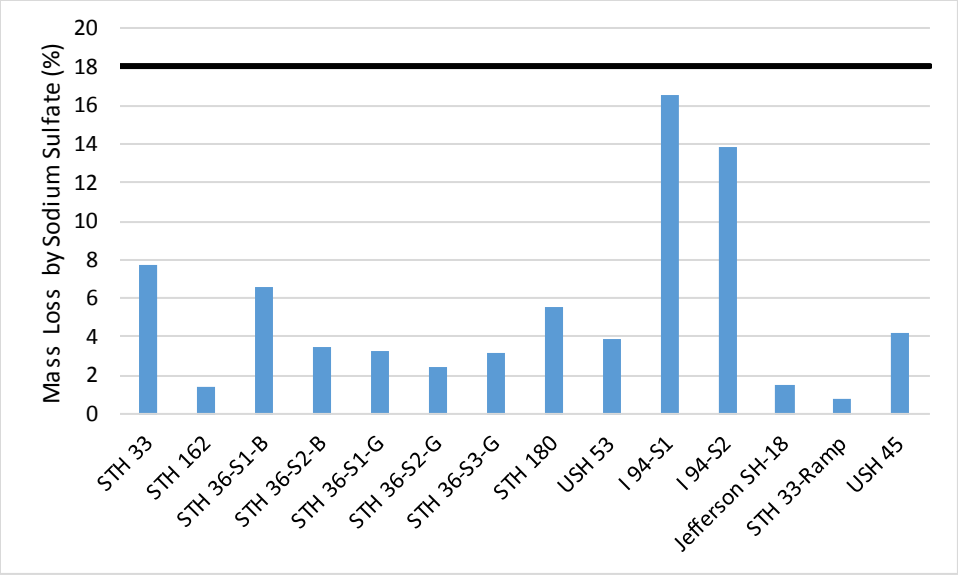

Figure 5.2: Bar graph displaying the results of the mass loss of coarse aggregates by sodium sulfate soundness and showing the WisDOT threshold of 18%.

The bar graph in Figure 5.3 shows the absorption of coarse aggregates. The coarse aggregate absorption values were compared with a target value of 2%. The base-course aggregates with absorption values that exceeded the recommended threshold limit were STH 33, STH 36-S1-B, STH 36-S2-G, STH 36-S3-G, I 94-S1, I 94-S2, and Jefferson SH-18. Therefore, seven of the fourteen collected samples exceeded the recommended threshold limit. Furthermore, six out of the eleven aggregates from existing base-course layers exceeded the recommended threshold limit.

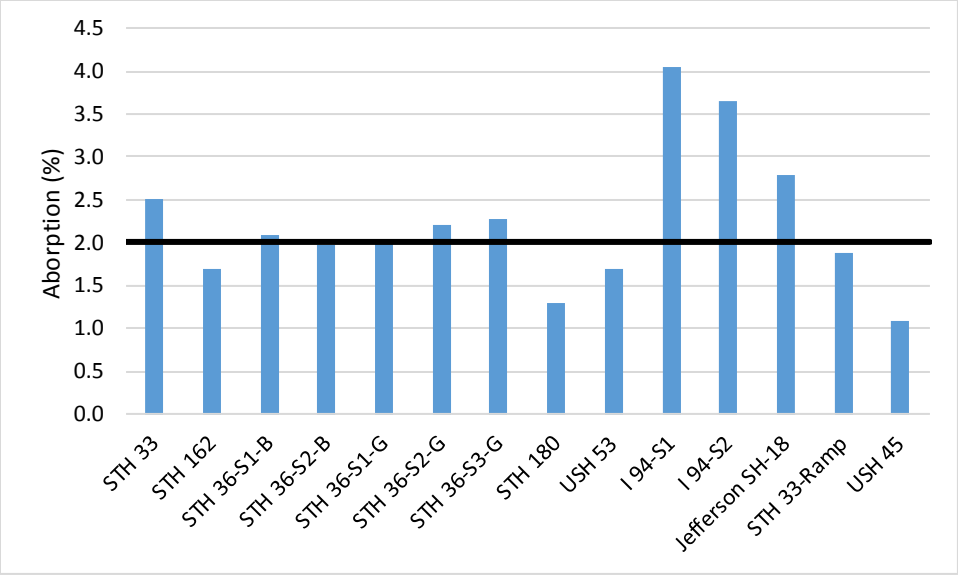

Figure 5.3: Bar graph displaying the results of the coarse aggregate absorption test and showing the recommended threshold value of 2%.

5.2 Regression Analyses of Sodium Sulfate Soundness versus Absorption

For sodium sulfate soundness versus absorption, the regression equation and coefficient of determination for each data set were compiled and displayed in Table 5.1. Regarding the graphs of sodium sulfate soundness versus absorption, only the graph that considered all data points combined was presented. Displaying the other graphs pertaining to the rest of the data sets for sodium sulfate soundness versus absorption was not necessary because the Micro-Deval abrasion versus absorption regression analyses showed stronger correlations than those analyzed for sodium sulfate versus absorption as can be seen later in this chapter.

Table 5.1: Regression equations and coefficients of determination for Sodium Sulfate versus Absorption.

Type	Regression Equation	R^2
VA-All (WHRP-1)	SS % Loss = 2.84 Absorption - 2.17	0.41
VA-Good (WHRP-1)	SS % Loss = 1.11 Absorption + 0.07	0.41
VA-Intermediate (WHRP-1)	SS % Loss = 0.55 Absorption + 2.53	0.03
VA-Poor (WHRP-1)	SS % Loss = 4.51 Absorption - 4.28	0.65
VA-Poor (WHRP-2)	SS % Loss = 3.73 Absorption - 5.69	0.15
VA-Mixed (WHRP-3)	SS % Loss = 1.33 Absorption + 0.91	0.12
Current Study	SS % Loss = 4.29 Absorption - 4.25	0.57
VA-All (WHRP-1, 2, & 3)	SS % Loss = 2.44 Absorption - 1.14	0.32
All Studies	SS % Loss = 2.53 Absorption - 1.22	0.33

The mass losses of coarse aggregate quantified by the sodium sulfate soundness test are plotted against coarse aggregate absorption as presented in Figure 5.4. The best fit line for the test data points is also shown in the figure. The mass loss by the sodium sulfate soundness test ranges between 0.06% (for coarse aggregate with 0.59% absorption) and 31.42% (for coarse aggregate with 5.87% absorption). For this graph, all data sets were combined to examine all aggregates from all of the studies considered. The plotted data demonstrated a relatively weak correlation between coarse aggregate absorption and mass loss by sodium sulfate soundness (R^2=0.33). Thus, it was reasonable to conclude that the regression equation cannot be used to accurately predict the mass loss of aggregates by sodium sulfate soundness from aggregate absorption. Three out of 123 coarse aggregates demonstrated by the graph exceeded the mass loss by sodium sulfate soundness threshold of 18% set by WisDOT.

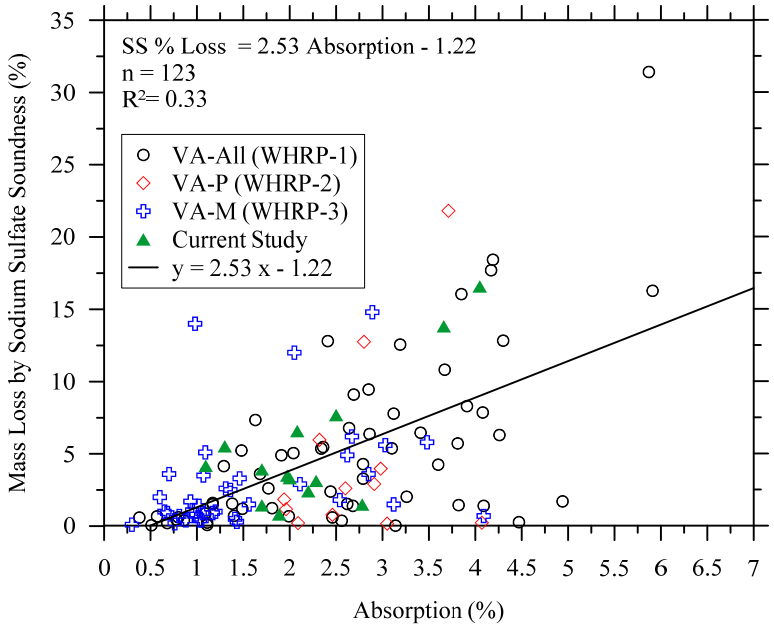

Figure 5.4: Comparison of mass loss of coarse aggregates by Sodium Sulfate Soundness versus coarse aggregate absorption for all studies (VA = Virgin Aggregate, P = Aggregate with poor performance, and M = Aggregate with mixed performance).

5.3 Regression Analyses of Sodium Sulfate Soundness versus Micro-Deval Abrasion

For sodium sulfate soundness versus Micro-Deval abrasion, the regression equation and coefficient of determination for each data set were compiled and displayed in Table 5.2. Regarding the graphs of sodium sulfate soundness versus Micro-Deval abrasion, only the graph that considered all data points combined was presented. Displaying the other graphs pertaining to the rest of the data sets for sodium sulfate soundness versus absorption was not necessary because the Micro-Deval abrasion versus absorption regression analyses showed stronger correlations than those analyzed for sodium sulfate versus absorption as can be seen later in this chapter. The results obtained regarding the correlations between sodium sulfate soundness and Micro-Deval abrasion indicating that the correlations were not strong between the two variables aligns with

Cooley's (2000) findings that there was no correlation between Micro-Deval abrasion and sodium sulfate soundness.

Table 5.2: Regression equations and coefficients of determination for Sodium Sulfate versus Micro-Deval.

Type	Regression Equation	R^2
VA-All (WHRP-1)	SS % Loss = 0.55 MD % Loss - 3.90	0.56
VA-Good (WHRP-1)	SS % Loss = 4.95 MD % Loss + 2.68	0.42
VA-Intermediate (WHRP-1)	SS % Loss = 0.22 MD % Loss + 0.38	0.13
VA-Poor (WHRP-1)	SS % Loss = 0.69 MD % Loss - 4.10	0.70
VA-Poor (WHRP-2)	SS % Loss = 0.66 MD % Loss - 11.00	0.53
VA-Mixed (WHRP-3)	SS % Loss = 0.12 MD % Loss + 1.19	0.05
Current Study	SS % Loss = 0.74 MD % Loss - 5.61	0.21
VA-All (WHRP-1, 2, & 3)	SS % Loss = 0.41 MD % Loss - 2.56	0.37
All Studies	SS % Loss = 0.41 MD % Loss - 2.32	0.34

The mass losses of coarse aggregate quantified by the sodium sulfate soundness test are plotted against the mass losses by Micro-Deval abrasion test as presented in Figure 5.5. The best fit line for the test data points is also shown in the figure. The mass loss by the sodium sulfate soundness test ranges between 0.06% (corresponding to mass loss by Micro-Deval abrasion 5.09%) and 31.42% (corresponding to mass loss by Micro-Deval abrasion 39.98%). For this graph, all data sets were combined to examine all aggregates from all of the studies considered. The plotted data demonstrated a relatively weak correlation between mass loss by Micro-Deval abrasion and mass loss by sodium sulfate soundness (R^2=0.34). Thus, it was reasonable to conclude that the regression equation cannot be used to accurately predict the mass loss of aggregates by sodium sulfate soundness from the mass loss of aggregates by Micro-Deval abrasion.

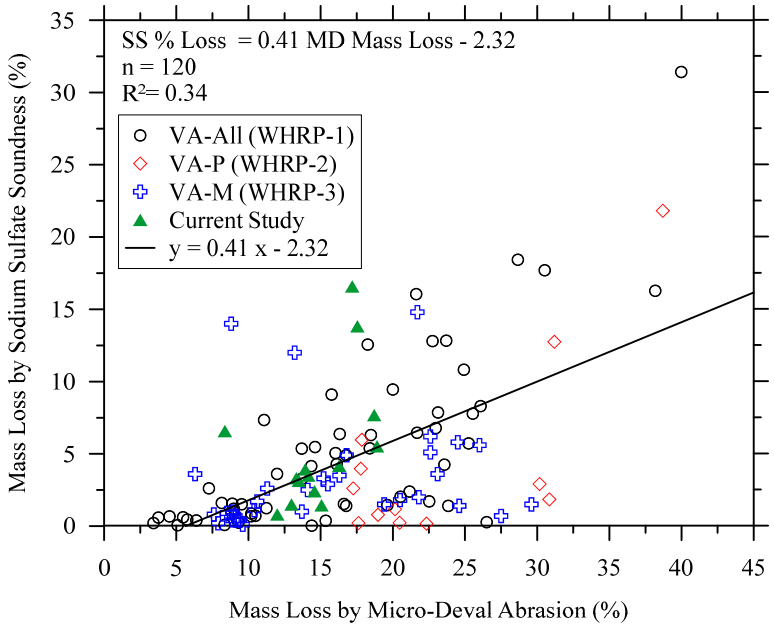

Figure 5.5: Comparison of mass loss of coarse aggregates by sodium sulfate soundness versus mass loss of coarse aggregates by Micro-Deval abrasion for all studies (VA = Virgin Aggregate, G = Aggregate with good performance, I = Aggregate with intermediate performance, P = Aggregate with poor performance, and M = Aggregate with mixed performance).

5.4 Regression Analyses of Micro-Deval Abrasion versus Absorption

This section presents the graphs produced for the regression analyses for Micro-Deval abrasion versus absorption for each of the data sets considered because the selected regression model was one of the regression equations relating mass loss by Micro-Deval abrasion and absorption.

The mass losses of coarse aggregate quantified by the Micro-Deval abrasion test are plotted against coarse aggregate absorption as presented in Figure 5.6. The best fit line for the test data points is also shown in the figure. The mass loss by the Micro-Deval abrasion test ranges between 3.42% (for coarse aggregate with 0.68% absorption) and 39.98% (for coarse aggregate with 5.87 % absorption). The data plotted in the figure

shows a strong correlation between coarse aggregate absorption and mass loss by Micro-Deval abrasion (R^2=0.86). This result agrees with the findings of Rismantojo about the existence of a significant relationship between Micro-Deval abrasion and aggregate absorption (Rismantojo 2000). Thus, it was reasonable to conclude that the regression equation can be used to accurately predict the mass loss of aggregates by Micro-Deval abrasion from aggregate absorption. From the coarse aggregates included in this graph, 22 out of 58 exceeded the recommended threshold of 18%.

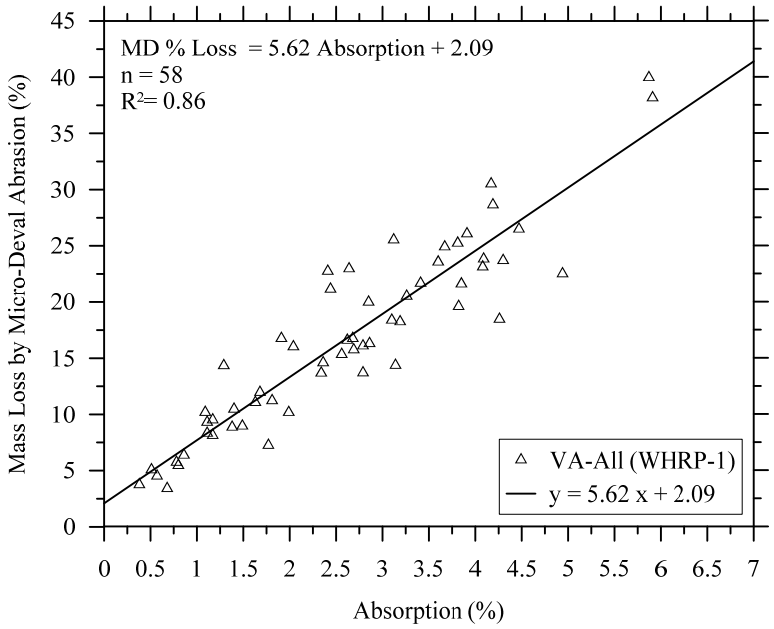

Figure 5.6: Comparison of mass loss of coarse aggregates by Micro-Deval Abrasion versus coarse aggregate absorption for all virgin aggregates from WHRP-1 (VA = Virgin Aggregate).

The mass losses of coarse aggregate quantified by the Micro-Deval abrasion test are plotted against coarse aggregate absorption as presented in Figure 5.7. The best fit lines for each of the three data sets shown are also shown in the figure.

For the virgin aggregates with good performance quality, the mass loss by the Micro-Deval abrasion test ranges between 3.76% (for coarse aggregate with 0.38% absorption) and 23.57% (for coarse aggregate with 3.6% absorption). The data plotted in the figure shows a strong correlation between coarse aggregate absorption and mass loss by Micro-Deval abrasion (R^2=0.87). Thus, it was reasonable to conclude that the regression equation can be used to accurately predict the mass loss of good aggregates by Micro-Deval abrasion from aggregate absorption. From the coarse aggregates included in this graph, 5 out of 20 exceeded the recommended threshold of 18%.

For the virgin aggregates with intermediate performance quality, the mass loss by the Micro-Deval abrasion test ranges between 3.42% (for coarse aggregate with 0.68% absorption) and 26.5% (for coarse aggregate with 4.47% absorption). The figure shows a relatively strong correlation between coarse aggregate absorption and mass loss by Micro-Deval abrasion (R^2=0.70). Thus, it was reasonable to conclude that the regression equation can be used to adequately predict the mass loss of intermediate aggregates by Micro-Deval abrasion from aggregate absorption. It is worth noting that the regression model is not as accurate as the previous two models. From the coarse aggregates included in this graph, 8 out of 25 exceeded the recommended threshold of 18%.

For the virgin aggregates with poor performance quality, the mass loss by the Micro-Deval abrasion test ranges between 5.09% (for coarse aggregate with 0.51% absorption) and 39.98% (for coarse aggregate with 5.87 % absorption). The figure shows a strong correlation between coarse aggregate absorption and mass loss by Micro-Deval

abrasion (R^2=0.92). Thus, it was reasonable to conclude that the regression equation can be used to accurately predict the mass loss of poor aggregates by Micro-Deval abrasion from aggregate absorption. It is worth noting that the sample size is small relative to the sample sizes considered in the previous graphs. From the coarse aggregates included in this graph, 10 out of 13 exceeded the recommended threshold of 18%.

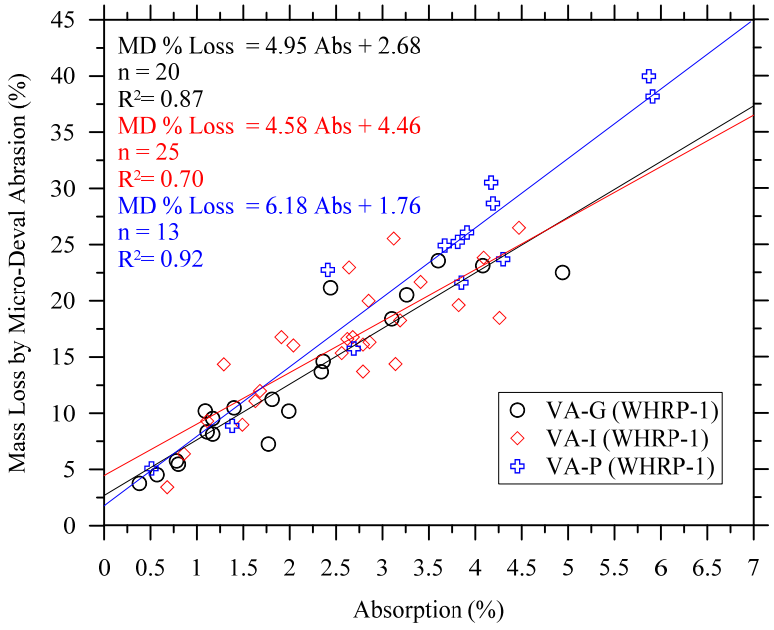

Figure 5.7: Comparison of mass loss of coarse aggregates by Micro-Deval Abrasion versus coarse aggregate absorption for good, intermediate, and poor virgin aggregates from WHRP-1 (VA = Virgin Aggregate, G = Aggregate with good performance, I = Aggregate with intermediate performance, and P = Aggregate with poor performance).

The mass losses of coarse aggregate quantified by the Micro-Deval abrasion test are plotted against coarse aggregate absorption as presented in Figure 5.8. The best fit line for the test data points is also shown in the figure. The mass loss by the Micro-Deval abrasion test ranges between 17.26% (for coarse aggregate with 2.6% absorption) and 38.7% (for coarse aggregate with 3.71% absorption). The data plotted in the figure shows

a weak correlation between coarse aggregate absorption and mass loss by Micro-Deval abrasion (R^2=0.09). Thus, it was reasonable to conclude that the regression equation cannot be used to accurately predict the mass loss of poor aggregates by Micro-Deval abrasion from aggregate absorption. From the coarse aggregates included in this graph, 8 out of 12 exceeded the recommended threshold of 18%.

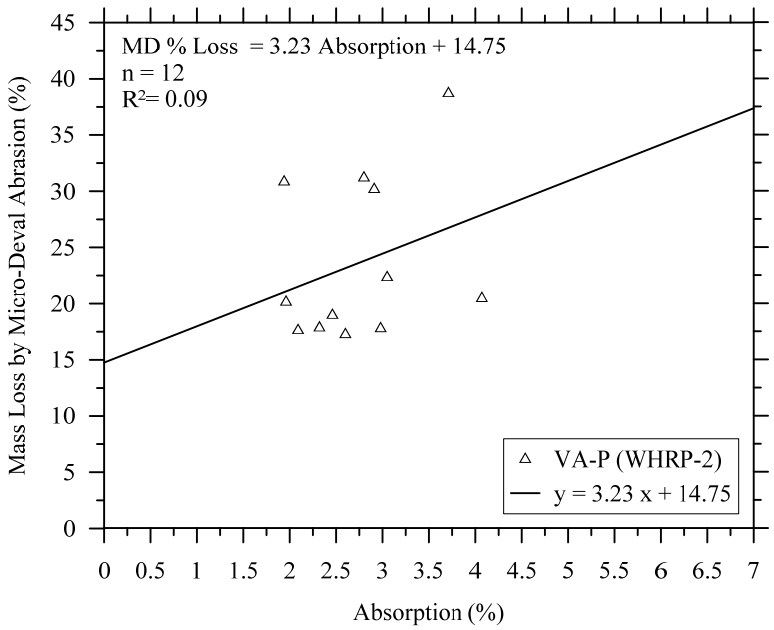

Figure 5.8: Comparison of mass loss of coarse aggregates by Micro-Deval Abrasion versus coarse aggregate absorption for poor virgin aggregates from WHRP-2 (VA = Virgin Aggregate, P = Aggregate with poor performance).

The mass losses of coarse aggregate quantified by the Micro-Deval abrasion test are plotted against coarse aggregate absorption as presented in Figure 5.9. The best fit line for the test data points is also shown in the figure. The mass loss by the Micro-Deval abrasion test ranges between 6.3% (for coarse aggregate with 0.7% absorption) and 27.5% (for coarse aggregate with 4.09% absorption). The data plotted in the figure shows a moderate correlation between coarse aggregate absorption and mass loss by Micro-

Deval abrasion (R^2=0.52). Thus, it was reasonable to conclude that the regression equation can be used to predict the mass loss of aggregates by Micro-Deval abrasion from aggregate absorption to some extent. From the coarse aggregates included in this graph, 12 out of 37 exceeded the recommended threshold of 18%.

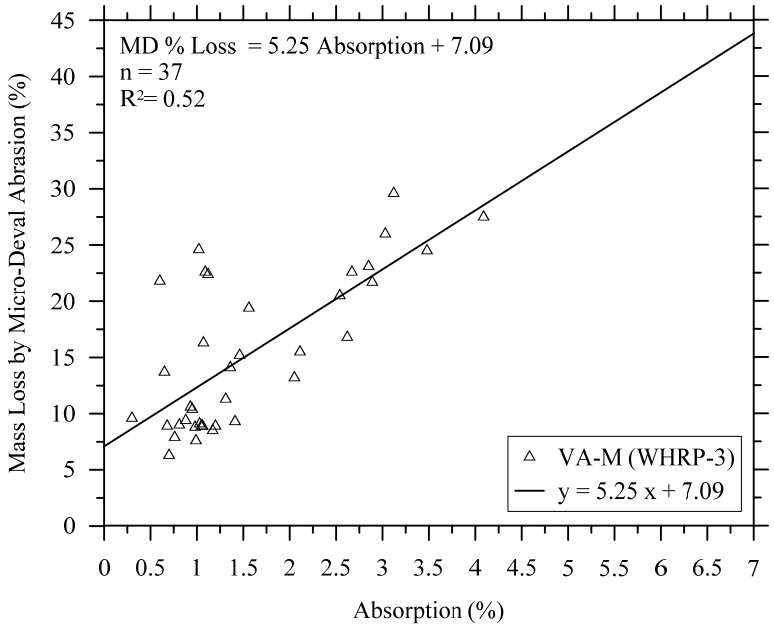

Figure 5.9: Comparison of mass loss of coarse aggregates by Micro-Deval Abrasion versus coarse aggregate absorption for mixed virgin aggregates from WHRP-3 (VA = Virgin Aggregate, M = Aggregate with mixed performance).

The mass losses of coarse aggregate quantified by the Micro-Deval abrasion test are plotted against coarse aggregate absorption as presented in Figure 5.10. The best fit line for the test data points is also shown in the figure. The mass loss by the Micro-Deval abrasion test ranges between 8.4% (for coarse aggregate with 2.08% absorption) and 18.9% (for coarse aggregate with 1.30% absorption). The data plotted in the figure shows a weak correlation between coarse aggregate absorption and mass loss by Micro-Deval abrasion (R^2=0.03). Thus, it was reasonable to conclude that the regression equation

cannot be used to accurately predict the mass loss of aggregates by Micro-Deval abrasion from aggregate absorption. Note that the sample size is relatively small. From the coarse aggregates included in this graph, 2 out of 14 exceeded the recommended threshold of 18%.

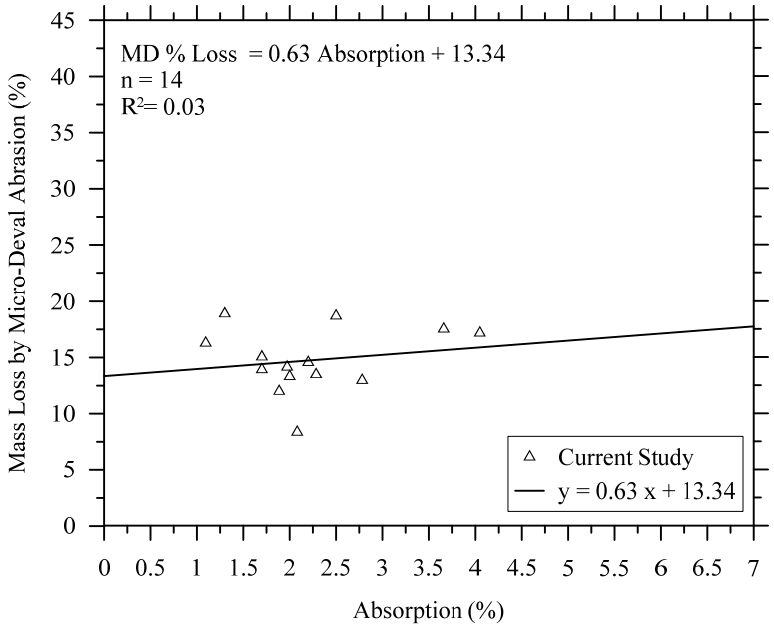

Figure 5.10: Comparison of mass loss of coarse aggregates by Micro-Deval Abrasion versus coarse aggregate absorption for mixed aggregates from the current study.

The mass losses of coarse aggregate quantified by the Micro-Deval abrasion test are plotted against coarse aggregate absorption as presented in Figure 5.11. The best fit line for the test data points is also shown in the figure. The mass loss by the Micro-Deval abrasion test ranges between 3.42% (for coarse aggregate with 0.68% absorption) and 39.98% (for coarse aggregate with 5.87 % absorption). The data plotted in the figure shows an adequately strong correlation between coarse aggregate absorption and mass loss by Micro-Deval abrasion (R^2=0.63). Thus, it was reasonable to conclude that the regression equation can be used to sufficiently predict the mass loss of virgin aggregates

by Micro-Deval abrasion from aggregate absorption. From the coarse aggregates included in this graph, 43 out of 107 exceeded the recommended threshold of 18%.

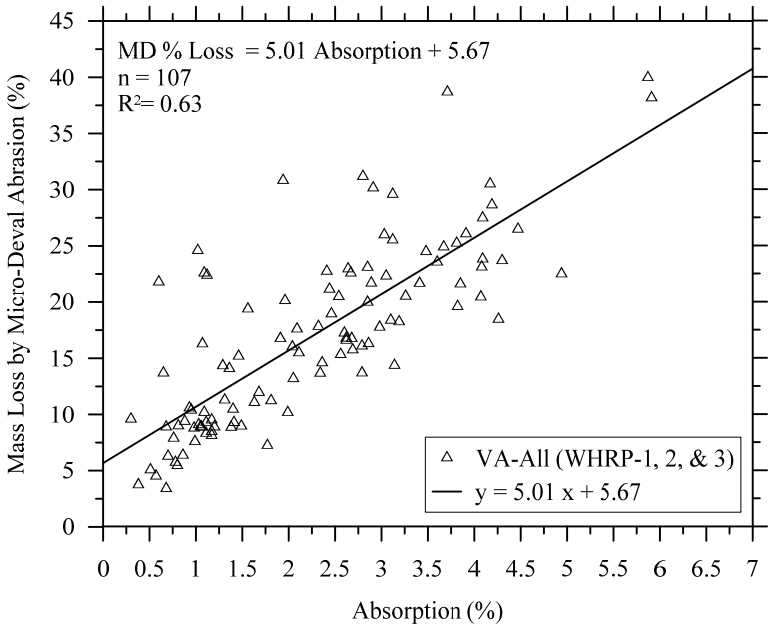

Figure 5.11: Comparison of mass loss of coarse aggregates by Micro-Deval Abrasion versus coarse aggregate absorption for virgin aggregates from WHRP-1, WHRP-2, and WHRP-3 (VA = Virgin Aggregate).

The mass losses of coarse aggregate quantified by the Micro-Deval abrasion test are plotted against coarse aggregate absorption as presented in Figure 5.12. The best fit line for the test data points is also shown in the figure. The mass loss by the Micro-Deval abrasion test ranges between 3.42% (for coarse aggregate with 0.68% absorption) and 39.98% (for coarse aggregate with 5.87 % absorption). The data plotted shows a moderately strong correlation between coarse aggregate absorption and mass loss by Micro-Deval abrasion (R^2=0.59). Thus, it was reasonable to conclude that the regression equation can be used to predict the mass loss of virgin aggregates by Micro-Deval abrasion from aggregate absorption to some extent. From the coarse aggregates included in this graph, 45 out of 121 exceeded the recommended threshold of 18%.

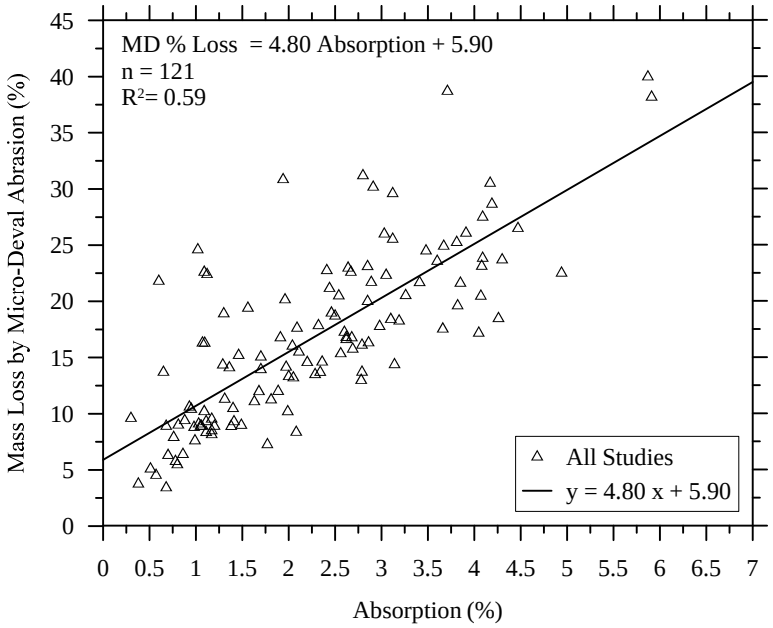

Figure 5.12: Comparison of mass loss of coarse aggregates by Micro-Deval Abrasion versus coarse aggregate absorption for all studies.

Figures 5.13 and 5.14 below display the same data plotted in Figure 5.12 except that the data are separated by performance quality in Figure 5.13 and by the study that the data originated from in Figure 5.14.

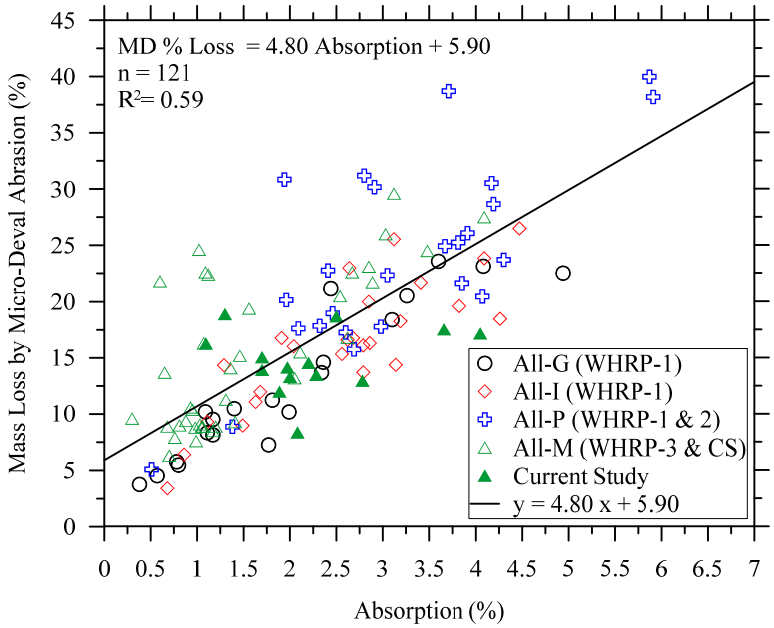

Figure 5.13: Comparison of mass loss of coarse aggregates by Micro-Deval Abrasion versus coarse aggregate absorption for all studies separated by aggregate quality (G = Aggregate with good performance, I = Aggregate with intermediate performance, P = Aggregate with poor performance, and M = Aggregate with mixed performance).

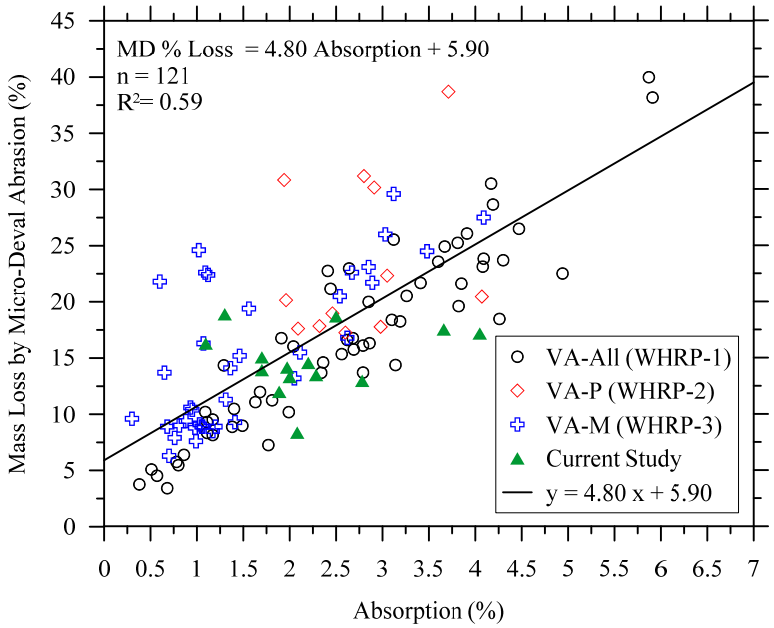

Figure 5.14: Comparison of mass loss of coarse aggregates by Micro-Deval Abrasion versus coarse aggregate absorption for all studies separated by study (VA = Virgin Aggregate, G = Aggregate with good performance, I = Aggregate with intermediate performance, P = Aggregate with poor performance, and M = Aggregate with mixed performance).

Table 5.3 summarizes the regression equations along with the coefficients of determination (R^2) obtained from the regression analyses performed on the various data sets shown in Figures 5.6 through 5.16. The regression equations with the strongest correlations are VA-Poor (WHRP-1), VA-Good (WHRP-1), and VA-All (WHRP-1) which had R^2 values of 0.92, 0.87, and 0.86 respectively. The samples sizes were 13 for VA-Poor (WHRP-1), 20 for VA-Good (WHRP-1), and 58 for VA-All (WHRP-1). The regression for VT Study-All was selected over the other two as the regression model to assess the aggregate quality of the samples that were examined in this specific study because not only did it have a strong correlation, but it also had a large sample size. The process of selecting the regression line also took into account the regression models developed for sodium sulfate versus absorption and sodium sulfate versus Micro-Deval. The largest value of R^2 for sodium sulfate versus absorption was 0.65 and the largest value of R^2 for sodium sulfate versus Micro-Deval was 0.70, while the R^2 value for the selected regression model was 0.86.

Table 5.3: Regression equations and coefficients of determination for Micro-Deval abrasion versus aggregate absorption.

Type	Regression Equation	R^2
VA-All (WHRP-1)	MD % Loss = 5.62 Absorption + 2.09	0.86
VA-Good (WHRP-1)	MD % Loss = 4.95 Absorption + 2.68	0.87
VA-Intermediate (WHRP-1)	MD % Loss = 4.58 Absorption + 4.46	0.70
VA-Poor (WHRP-1)	MD % Loss = 6.18 Absorption + 1.76	0.92
VA-Poor (WHRP-2)	MD % Loss = 3.23 Absorption + 14.75	0.09
VA-Mixed (WHRP-3)	MD % Loss = 5.25 Absorption + 7.09	0.52
Current Study	MD % Loss = 0.63 Absorption + 13.34	0.03
VA-All (WHRP-1, 2, & 3)	MD % Loss = 5.01 Absorption + 5.67	0.63
All Studies	MD % Loss = 4.80 Absorption + 5.90	0.59

The graph depicted in Figure 5.15 shows two lines of best fit, one for All Studies and the other for WHRP-1. The reason that the regression line for All Studies is displayed on the graph is because this graph consists of the data points from all of the studies. WHRP-1 was selected as the regression model that was used to assess the aggregate quality of the samples that were examined in this specific study. The regression equation for WHRP-1 is MD % Loss = 5.62 Absorption + 2.09.

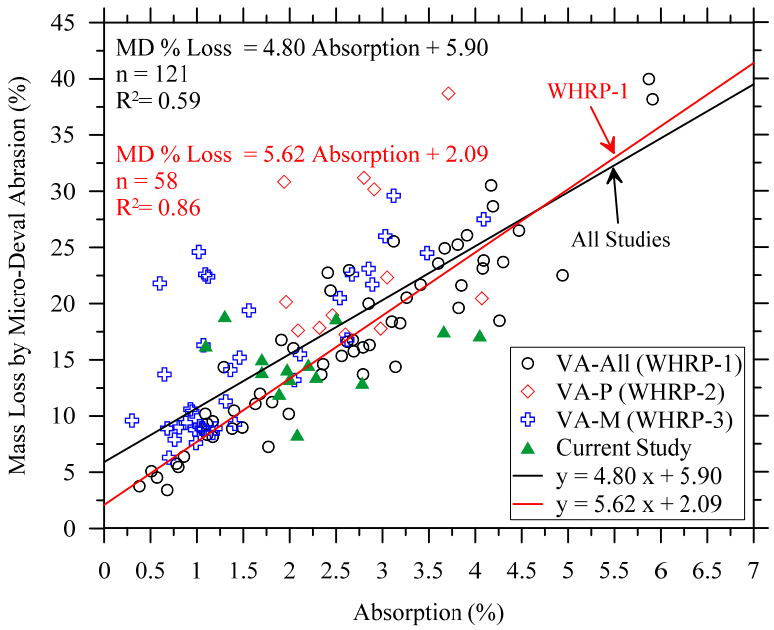

Figure 5.15: Comparison of mass loss of coarse aggregates by Micro-Deval Abrasion versus coarse aggregate absorption for all studies with regression lines of All Studies and WHRP-1 (VA = Virgin Aggregate, G = Aggregate with good performance, I = Aggregate with intermediate performance, P = Aggregate with poor performance, and M = Aggregate with mixed performance).

Figure 5.16 displays the regression line of all virgin aggregates from WHRP-1 presented in Figure 5.15. The data set from the current study is the only set of points shown on the graph so that the individual points could be compared with the selected regression line (WHRP-1). The individual points are labeled to indicate which project site each specific point originated from.

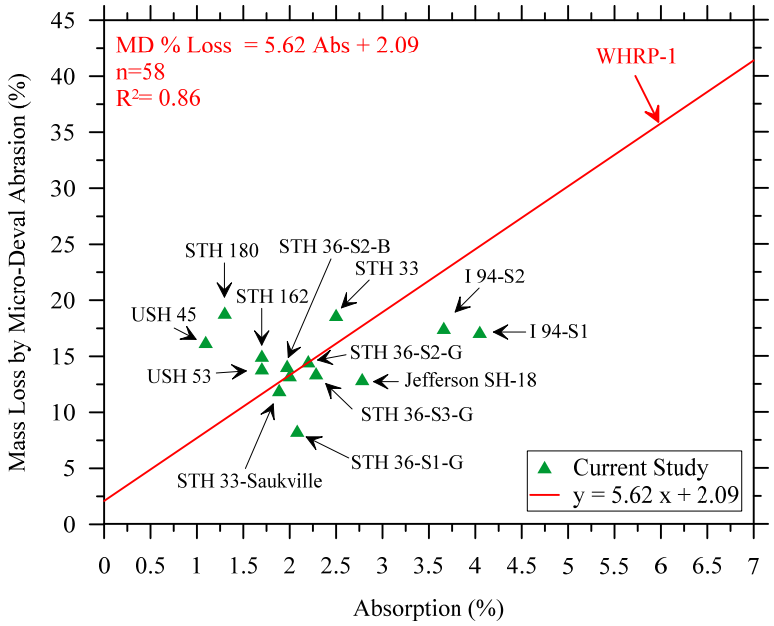

Figure 5.16: Regression line of Micro-Deval Abrasion loss versus coarse aggregate absorption for WHRP-1 with labels for the site location of each point.

It was reasonable to assume that the points above the line indicated potentially poor performance, and the points below the line indicated good performance. It was assumed that points above the selected regression line were aggregates with potentially poor performance, and it was assumed that points that were below the selected regression line were aggregates with good performance.

The points above the selected regression line represent the samples from the following project sites: STH 33, STH 162, STH 36-S2-B, STH 36-S2-G, STH 180, USH 53, and USH 45. The points below the selected regression line represent the samples from the following project sites: STH 36-S1-B, STH 36-S1-G, STH 36-S3-G, I 94-S1, I 94-S2, Jefferson SH-18, and STH 33-Saukville. Half of the aggregates from this specific study indicated potentially poor performance according to the selected prediction model. Out of

Furthermore, six out of the eleven aggregates from existing base-course layers indicated potentially poor performance. Revisiting Figure 5.17, approximately 53% of aggregates from all studies indicated potentially poor performance according to the selected prediction model.

5.5 Comparison of Estimated CBR with Soaked CBR

The average CBR of the base layer estimated from Kleyn's equation were compared to the soaked CBR values that were calculated from the CBR test data. The estimated CBR from the DCP test results along with the estimation of the base-course layer thicknesses are presented in Figure 5.12 through Figure 5.22. The figures also compare the soaked CBR values with the estimated CBR and they typically were in agreement with each other.

In Figure 5.17, the soaked CBR was 58.0 and the estimated CBR values of the base layer ranged from 32.7 to 73. The estimated CBR values were both higher than the soaked CBR value. The estimated CBR values of Test 1 and Test 2 were higher than the soaked CBR value. The estimated CBR value of Test 3 was lower than the soaked CBR value.

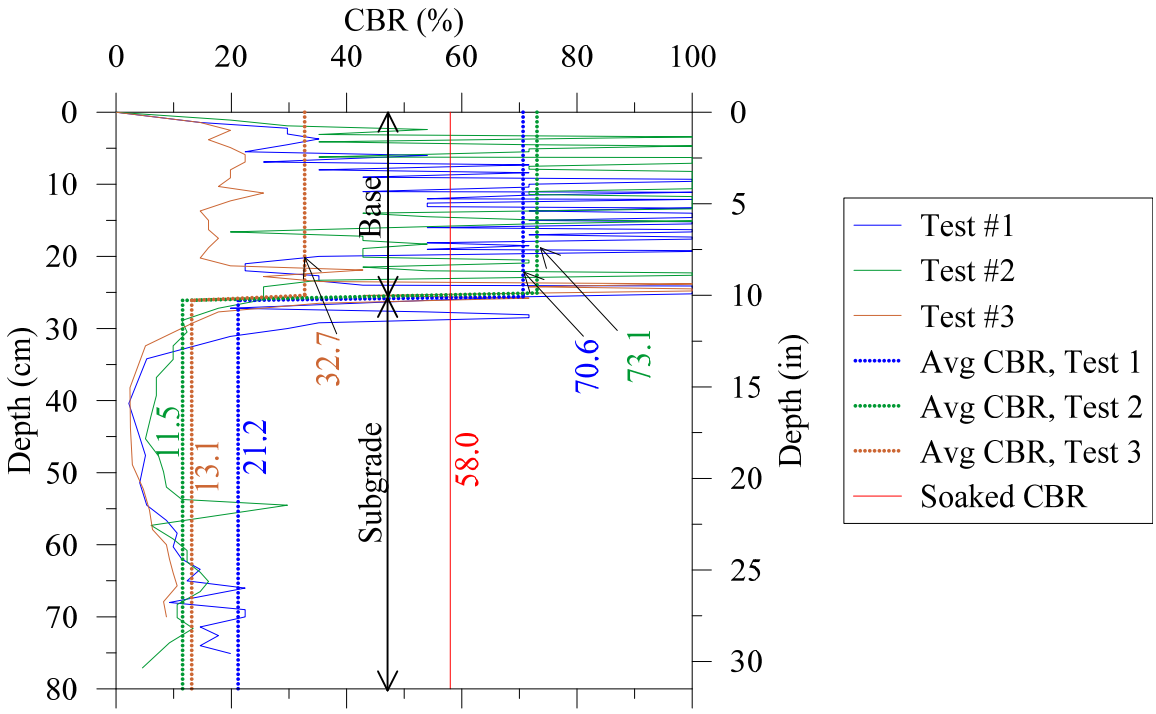

Figure 5.17: Average CBR values estimated from Kleyn's equation compared to the soaked CBR value for STH 33.

In Figure 5.18, the soaked CBR was 55.1 and the estimated CBR values for the base layer were 50.1 and 95.8. The estimated CBR values of Test 1 was lower than the soaked CBR value, and the estimated CBR value of Test 2 was higher than the soaked CBR value.

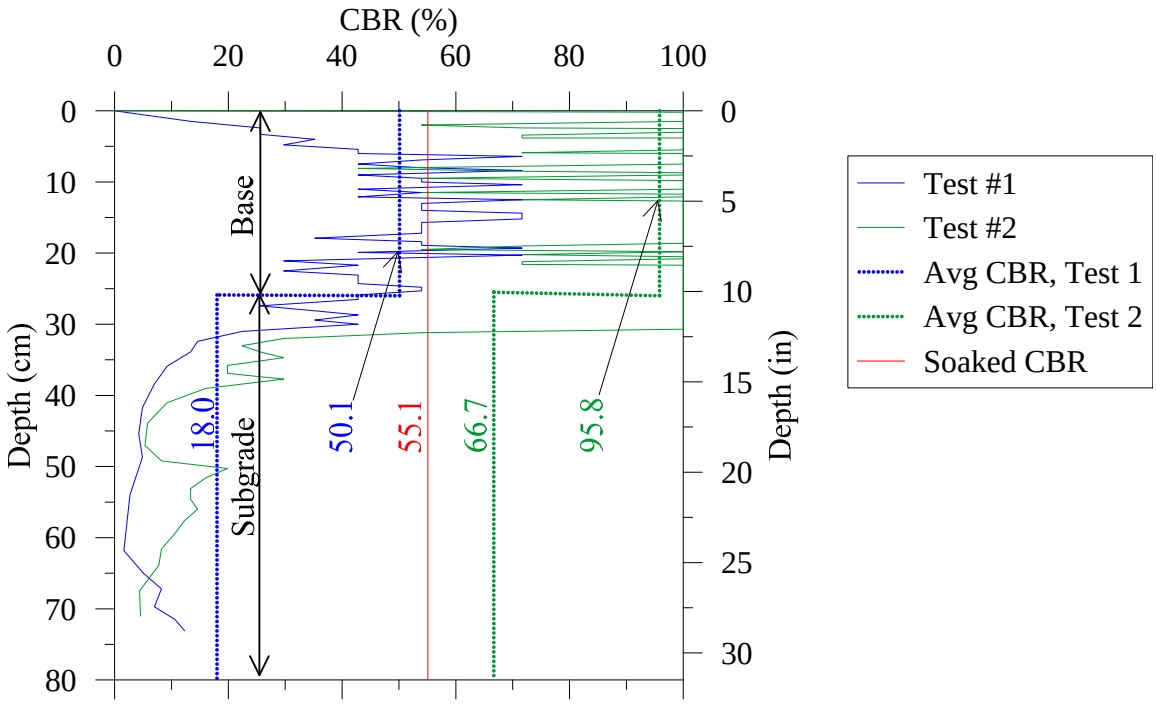

Figure 5.18: Average CBR values estimated from Kleyn's equation compared to the soaked CBR value for STH 162.

In Figure 5.19, the soaked CBR was 87.0 for the brown aggregate and the estimated CBR values ranged from 42.8 to 64.6 for the base layer. The estimated CBR values were lower than the soaked CBR value for the brown aggregate. The soaked CBR was 53.6 for the gray aggregate and the estimated CBR ranged from 28.1 to 33.7. The estimated CBR values were lower than the soaked CBR value for the gray aggregate.

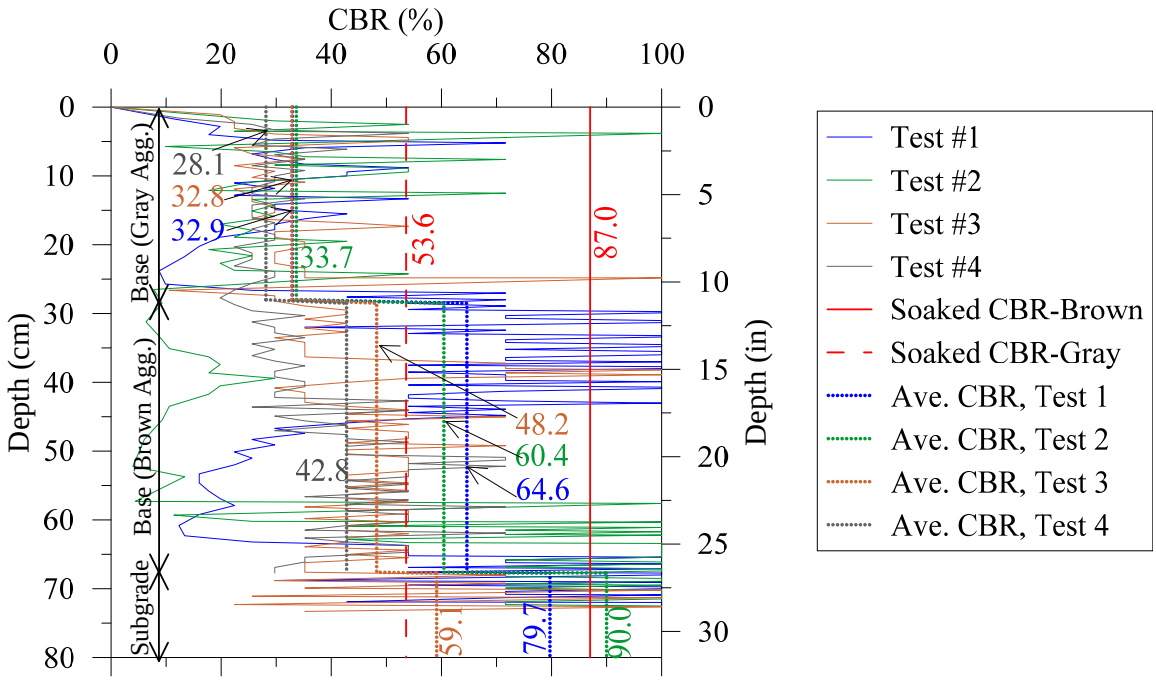

Figure 5.19: Average CBR values estimated from Kleyn's equation compared to the soaked CBR value for STH 36-S1.

In Figure 5.20, the soaked CBR was 21.7 for the gray aggregate and the estimated CBR values for the base layer were 38.4 and 71.2. The estimated CBR values were higher than the soaked CBR value for the gray aggregate. As a note, the brown aggregate was not included in the DCP test due to the removal of the brown aggregate layer before the DCP test was performed on this site.

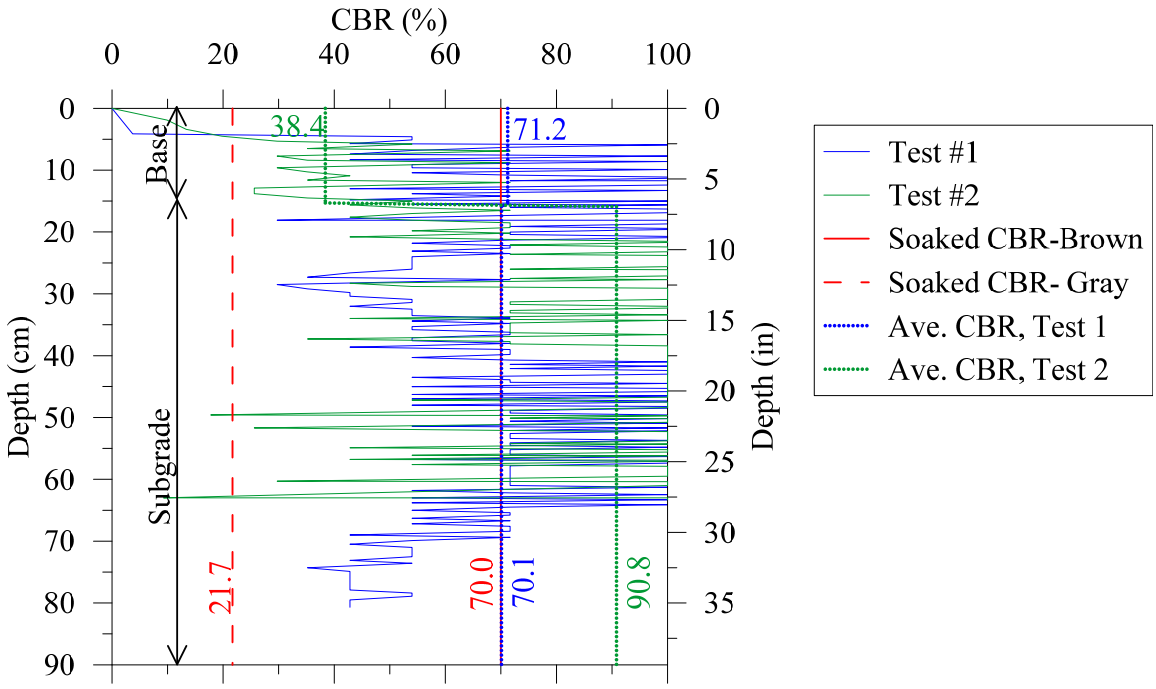

Figure 5.20: Average CBR values estimated from Kleyn's equation compared to the soaked CBR value for STH 36-S2.

In Figure 5.21, the soaked CBR was 89.9 for the gray aggregate and the estimated CBR values for the base layer were 42.2 and 44.8. The estimated CBR values were lower than the soaked CBR. As a note, the brown aggregate was not included in the DCP test due to the removal of the brown aggregate layer before the DCP test was performed on this site.

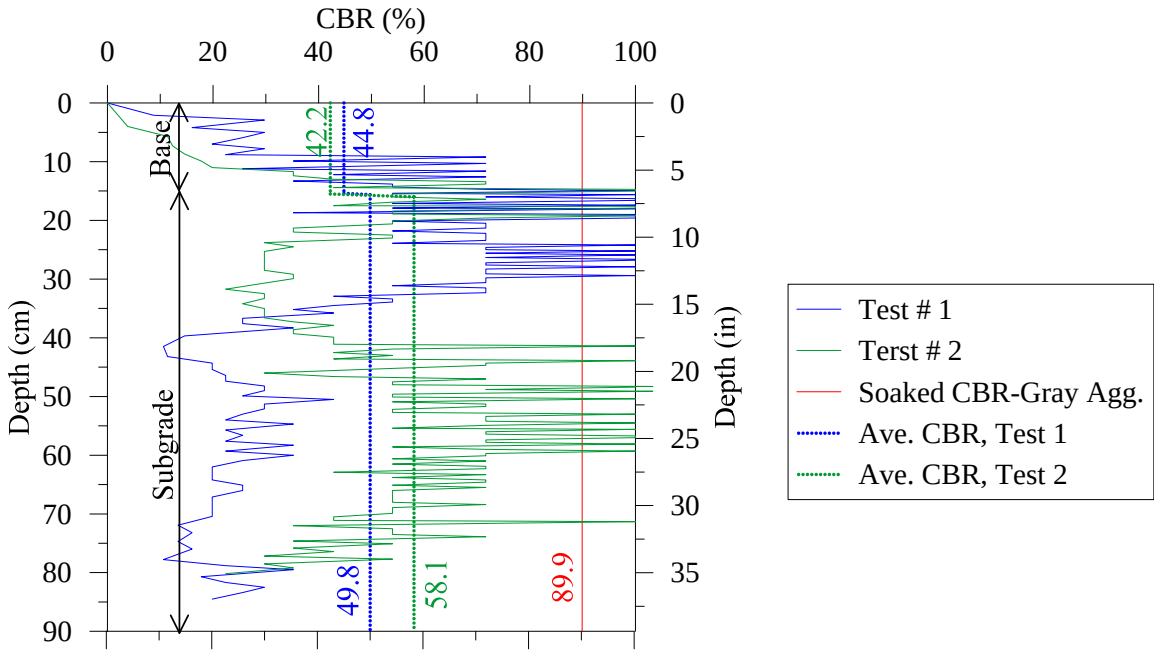

Figure 5.21: Average CBR values estimated from Kleyn's equation compared to the soaked CBR value for STH 36-S3.

In Figure 5.22, the soaked CBR was 56.7. The estimated CBR values ranged from 28.8 to 54.7. The estimated CBR values were both lower than the soaked CBR.

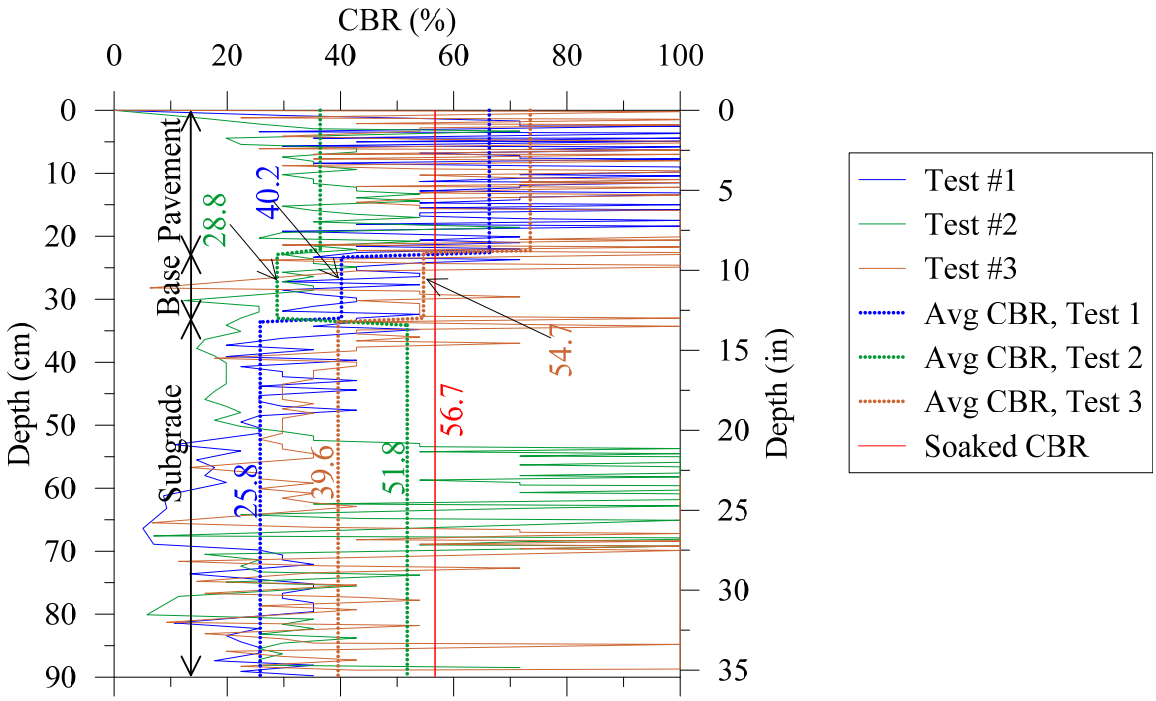

Figure 5.22: Average CBR values estimated from Kleyn's equation compared to the soaked CBR value for STH 180.

In Figure 5.23, the soaked CBR was 43.5. The estimated CBR values for the base layer were 20.1 and 22.6. The estimated CBR values both were lower than the soaked CBR.

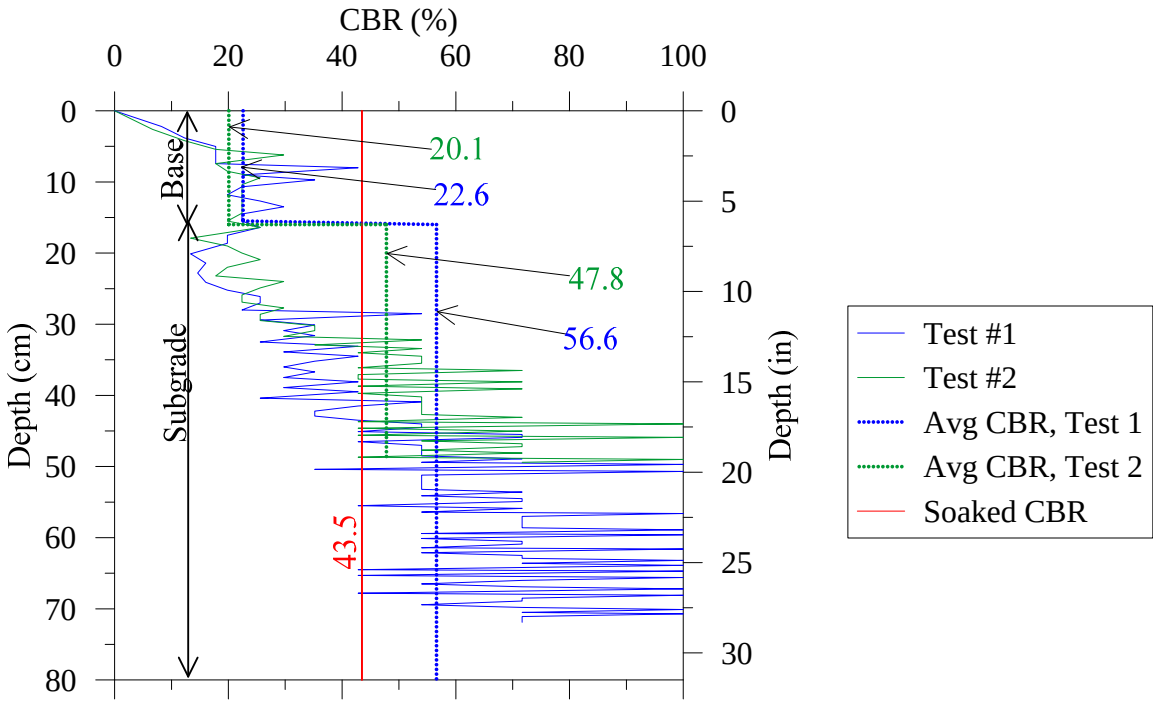

Figure 5.23: Average CBR values estimated from Kleyn's equation compared to the soaked CBR value for USH 53.

In Figure 5.24, the soaked CBR were 76.7 for I 94-S1 and 73.9 for I 94-S2. The DCP test was not performed on I 94-S1, so there were no estimated CBR values for I 94-S1. The estimated CBR values for the base layer were 64.2 and 67.2 for I 94-S2. The estimated CBR values for I 94-S1 were lower than both soaked CBR values shown in the figure.

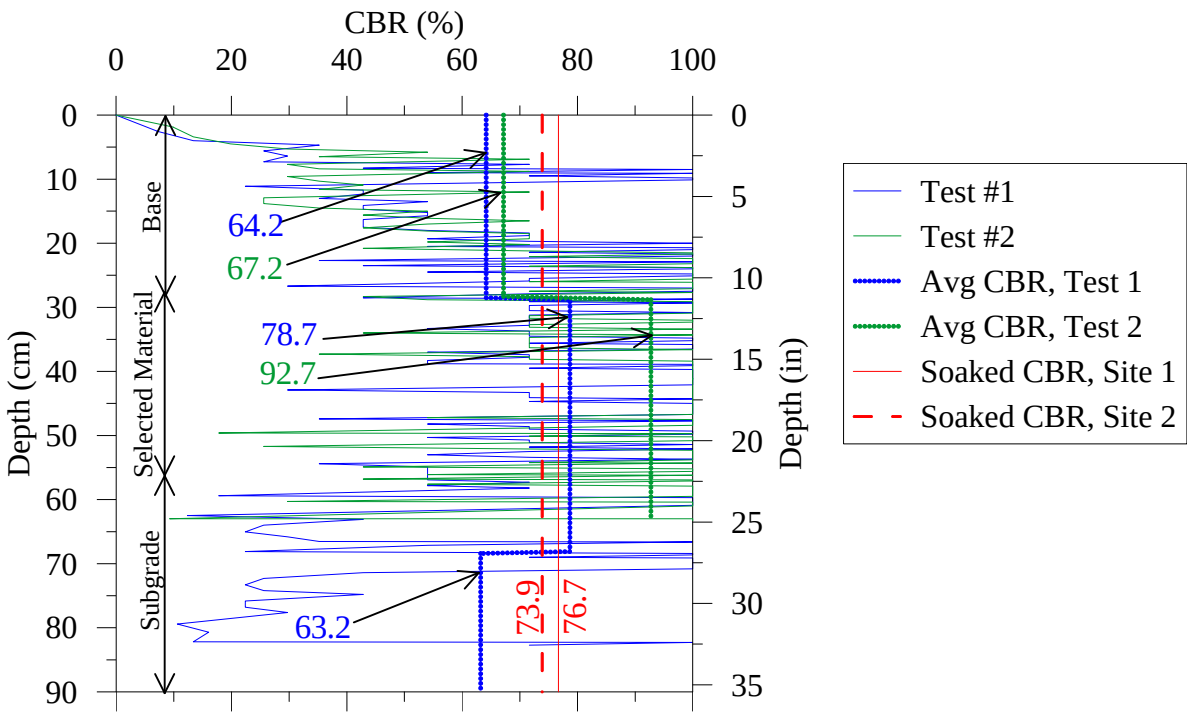

Figure 5.24: Average CBR values estimated from Kleyn's equation for I 94-S2 compared to the soaked CBR values for I 94-S1 and I 94-S2.

CHAPTER 6

CONCLUSIONS

This research investigated the durability of aggregates in existing base-course layers in Wisconsin pavements. Aggregate samples were collected from various pavement project locations in Wisconsin and were subjected to laboratory tests including the Micro-Deval abrasion, sodium sulfate soundness, and aggregate absorption tests. Moreover, relevant data sets from other studies were obtained and used for analysis in combination with the data obtained from the samples collected for this thesis. In this study, additional parameters were provided to accurately identify the sites and materials where the samples were obtained from. These parameters included map locations, GPS coordinates, layer thicknesses, and ages of layers. The layer thicknesses were obtained from project plans, field measurements, and from the DCP test results.

The results of the Micro-Deval abrasion, sodium sulfate soundness, and absorption tests were compared with recommended threshold limits to draw conclusions about where the collected samples stood relative to the WisDOT and recommended threshold limits. The results of those tests demonstrated the following conclusions:

1) The Micro-Deval abrasion test results showed that two of the fourteen collected samples exceeded the recommended threshold limit of 18%. Of the eleven collected samples that were aggregates from existing base-course layers, two samples exceeded the recommended threshold limit.

2) The sodium sulfate soundness test results showed that none of the fourteen collected samples exceeded the WisDOT threshold limit of 18%. Thus, none of the aggregates from existing base-course layers exceeded the threshold limit.
3) The absorption test results showed that seven of the fourteen collected samples exceeded the recommended threshold limit of 2%. Of the eleven of the collected samples that were aggregates from existing base-course layers, six of those eleven samples exceeded the recommended threshold limit.

The regression analyses of the results generated from the combined data (data obtained from collected samples for this study and the data obtained from the other studies) led to drawing the following conclusions.

1) The regression model MD % Loss = 5.62 × Absorption + 2.09, with an R^2 value of 0.86, can be used to make predictions with a high level of accuracy. The term "MD % Loss" in the regression equation represents percent loss by the Micro-Deval abrasion test and the term "Absorption" represents aggregate absorption.
2) The regression model MD % Loss = 5.62 × Absorption + 2.09 can be used to assess the performance quality of base-course aggregates. According to this model, seven of the fourteen collected samples were above the regression line and these aggregates were assumed to have the potential for exhibiting poor performance on the basis of this model. Out of the eleven aggregates that were from existing base-course layers, six were above the regression line and these aggregates were assumed to have the potential for exhibiting poor performance on the basis of this model.

3) The mass loss by sodium sulfate soundness did not have strong correlations with either absorption or the mass loss of Micro-Deval abrasion. Because of this, the regression lines developed are not accurate indicators of aggregate quality. Accordingly, it may be of interest to use the unconfined freeze-thaw test or the freeze-thaw soundness test to assess the freeze-thaw durability and to see if there is a correlation between either of those tests and absorption.

In addition to the durability-related tests that were performed in this study, strength-related tests were conducted. The combination of the results of these tests can be used a as a frame of reference for a more comprehensive performance assessment of base-course aggregates.

REFERENCES

1. ASTM, 2016, "*Annual Book of ASTM Standards*." Vol. 04.02, ASTM, Philadelphia, PA.

2. ASTM, 2016, "*Annual Book of ASTM Standards*." Vol. 04.03, ASTM, Philadelphia, PA.

3. ASTM, 2016 "*Annual Book of ASTM Standards*." Vol. 04.08, ASTM, Philadelphia, PA.

4. Bluman, A. (2004). *Elementary Statistics* (5th ed.). New York, NY: McGraw-Hill.

5. Cooley, L. J., Jr., Hunter, M. S., & James, R. S. (2002). *Micro-Deval Testing of Aggregates in The Southeast* (pp. 1-28, Rep. No. NCAT # 02-09). Auburn, AL: NCAT.

6. DOT, W. (2017). *Facilities Development Manual (FDM)*. Retrieved May 08, 2017, from http://wisconsindot.gov/Pages/doing-bus/eng-consultants/cnslt-rsrces/rdwy/fdm.aspx.

7. Google Maps. (2017). [Map of Wisconsin]. Retrieved April 10, 2017, from https://www.google.com/maps/place/Wisconsin/@44.7643424,-92.0695726,7z/data=!3m1!4b1!4m5!3m4!1s0x52a8f40f9384e3af:0xf2d5d5b8f88649d6!8m2!3d43.7844397!4d-88.7878678.

8. Hossain, M., Lane, D., & Schmidt, B. (2007). *Use of the Micro-Deval Test for Assessing the Durability of Virginia Aggregates* (VTRC 07-R29). Charlottesville, VA: Virginia Transportation Research Council.

9. Hunt, E. L. (2001). *Micro-Deval Coarse Aggregate Test Evaluation: Final Report* (OR-RD-01-13). Retrieved from Oregon Department of Transportation Research.

10. Jigar, S., & Patel, A. (2013). *Comparison between Soaked and Unsoaked CBR*. International Journal of Advanced Engineering Research and Studies, 2(3), 1-4.

11. Kandhal, P. S., & Parker Jr., F. (1998). *Aggregate Tests Related to Asphalt Concrete Performance in Pavements* (405).

12. Pigeon, M., & Pleau, R. (1995). *Durability of Concrete in Cold Climates*. Boca Raton, FL: CRC.

13. Rismantojo, E. "*Permanent Deformation and Moisture Susceptibility Related Aggregate Tests for Use in Hot -Mix Asphalt Pavements*". Ph.D. Purdue University, 2002.

14. Tabatabai, H., Titi, H., Lee, C., Qamhia, I., & Fella, G. P. (2013). *Investigation of Testing Methods of Determine Long-Term Durability of Wisconsin Aggregates* (pp. 1-77, Rep.). WI: Wisconsin Highway Research Program.

15. Titi, H., Tabatabi, H., Bautista, E., & Druckrey, A. (2012). *Base Compaction Specification Feasibility Analysis* (WHRP). Department of Civil Engineering and Mechanics.

16. Weyers, R. E., Williamson, G. S., Mokarem, D. W., Lane, D. S., & Cady, P. D. (2005). *Testing Methods to Determine Long Term Durability of Wisconsin Aggregate Resources* (pp. 1-58, Rep. No. WHRP 06-07). WI: Wisconsin Highway Research Program.

17. Wijekoon, W. (2014). *Investigation of A Relationship Between Soaked CBR And DCP CBR Value for Different Types of Soils* (Master's thesis, University of Moratuwa of Sri Lanka). University of Moratuwa of Sri Lanka.

18. Woodward, W. (1995). *Laboratory Prediction of Surfacing Aggregate Performance*. Doctoral dissertation. University of Ulster, Ireland.

19. Wu, Y., Parker, F., & Kandhal, K. (1998). *Aggregate Toughness/Abrasion Resistance and Durability/Soundness Tests Related to Asphalt Concrete Performance in Pavements* (98-4). Auburn University, AL: National Center for Asphalt Technology.